AIDS RESEARCH AND HUMAN RETROVIRUSES
Volume 23, Number 1, 2007, pp. 43–50

DOI: 10.1089/aid.2006.0029

Short Communication

Reversal Periods and Patterns from Drug-Resistant to Wild-Type HIV Type 1 after Cessation of Anti-HIV Therapy

XIUQIONG BI,[1,2] HIROYUKI GATANAGA,[1] KAZUHIKO KOIKE,[2] SATOSHI KIMURA,[1] and SHINICHI OKA[1]

ABSTRACT

Anti-HIV drug-resistant virus reverts to wild type following discontinuation of antiretroviral therapy (ART). This study aimed to determine the reversal period. ART was discontinued in 16 patients harboring drug-resistant viruses. Resistant mutations of reverse transcriptase (RT) and protease (PR) genes of plasma- and peripheral blood mononuclear cells (PBMC)-derived viruses were examined by direct sequencing monthly until the disappearance of mutants (median follow-up period: 8.9 months). Only wild-type virus was detected in 50% of patients at 6.3 months (quartiles, 3.2–20.7 months) and at 9.2 months (quartiles, 5.7–13.8 months) in plasma- and PBMC-derived viruses, respectively, after ART interruption. Among the 133 resistance-associated mutations identified at ART interruption, half the RT and PR mutations shifted to wild type in 3.2 months in plasma, 6.7 months of RT, and 5.7 months of PR in PBMC, respectively. In plasma- and PBMC-derived viruses, the PR mutations reverted earlier than the RT mutations. These results could be relevant as to when to perform drug-resistance testing.

THE EMERGENCE OF DRUG-RESISTANCE-ASSOCIATED MUTATIONS leads to treatment failure and may limit future treatment options. Therefore, inclusion of drug-resistance testing is recommended in anti-HIV-1 treatment guidelines, especially after failure of standard regimens.[1,2] A number of studies showed that drug-resistance testing improved the benefits of antiretroviral therapy (ART).[3–8] For drug resistance testing, plasma and peripheral blood mononuclear cell (PBMC) can be used as clinical specimens.[9] Using direct sequencing, we reported previously the earlier detection of resistant mutations in plasma than in PBMC.[10] Accordingly, we recommended the use of plasma for early detection of drug resistance during therapy in those patients who fail to respond to antiretroviral treatment. Clinically, even when patients develop virologic failure [rebound of plasma HIV-1 viral load (VL)], the CD4 count remains sufficiently high for treatment interruption, at least in some patients. In such cases, the timing of genotypic drug resistance testing is of practical importance. Discontinuation of treatment causes the reversion of resistance mutations to wild-type viruses.[11–18] Previous studies indicated that resistance mutations of plasma viruses could rapidly become undetectable either partially or entirely from 14 days to 4 months after ART cessation.[12–18] The reversion of mutations to wild type is considered to be due to the low replication fitness of mutant variants and outgrowth of wild type viruses when the drug-selective pressure is withdrawn.[17,21–22] However, the time course and pattern of this reversion have not been studied in detail in heavily treated patients. Clarification of this issue will help determine the most appropriate time and sample for performing genotypic-resistance testing after ART cessation.

The study subjects were 16 HIV-1-infected patients who had been known to have drug-resistance virus beforehand and discontinued antiretroviral therapy from August 1998 through December 2002 for a variety of reasons. All patients regularly consulted the AIDS Clinical Center at the International Medical Center of Japan, Tokyo, and gave written informed consent. Their demographic data and clinical characteristics at the time of quitting ART are listed in Table 1. Their blood samples were

[1]AIDS Clinical Center, International Medical Center of Japan, Tokyo, Japan.
[2]Graduate School of Medicine, University of Tokyo, Tokyo, Japan.

TABLE 1. DEMOGRAPHIC AND CLINICAL CHARACTERISTICS OF PATIENTS[a]

Pt	*Sex*	*Age (years)*	*Risk factor*	*CD4 cells/μl*	*log_{10} VL month 0*	*log_{10} VL month 1*	*Duration of ART (months)*	*Drugs ever used*	*Reasons of ART stop*
1	M	40	Bisexual	404	5.2	5.3	70.4	AZT, 3TC, d4T, ddI, NFV, RTV, SQH	Virological failure
2	M	23	Hemophilia	103	5	5	46.6	ddC, d4T, 3TC, AZT, ddI, SQH, NFV, IDV	Virological failure
3	M	36	MSM	209	3.5	3.5	91.8	AZT, 3TC, d4T, ddI, NFV	Virological failure
4	M	22	Hemophilia	116	5.1	4.3	71.9	ddC, d4T, 3TC, ABC, ddI, AZT, EFV, SQH, NFV, APV	Virological failure
5	M	26	Hemophilia	30	5.7	5.2	50.2	d4T, 3TC, ddI, AZT, NFV, IDV, RTV	Virological failure
6	M	28	Hemophilia	93	3.6	3.7	129.7	d4T, ddI, AZT, 3TC, ABC, ddC, EFV, RTV, SQH, IDV, NFV, APV	Virological failure
7	M	29	Hemophilia	698	1.7	5	108.6	AZT, 3TC, d4T, ddI, ABC, EFV, RTV, SQH	Side effects
8	M	24	Hemophilia	35	5.1	5.1	67	AZT, 3TC, ddC, SQH, RTV	Virological failure
9	F	42	Heterosexual	690	1.8	4.4	90	AZT, ddI, d4T, 3TC, ABC, EFV, SQH, APV, NFV	Poor adherence
10	M	19	Hemophilia	586	1.8	4.2	107.6	AZT, ddC, d4T, 3TC, ddI, ABC EFV, IDV, RTV, NFV, SQH, LPV/r	Poor adherence
11	M	24	Hemophilia	644	1.7	4.5	117.6	AZT, ddI, 3TC, IDV, RTV	Poor adherence
12	M	22	Hemophilia	138	4.5	4.5	53.4	AZT, ddC, d4T, 3TC, ddI, NVP, SQH, RTV, IDV	Virological failure
13	M	34	Bisexual	276	1.7	3.6	47.6	d4T, 3TC, ddI, ABC, AZT, NFV, IDV, RTV, LPV/r	Poor adherence
14	M	42	MSM	420	4.3	5.3	49.8	AZT, 3TC, d4T, ddI, IDV, RTV, SQH	Virological failure
15	M	39	Hemophilia	544	1.7	4.5	140.8	AZT, d4T, 3TC, NVP, NFV	Side effects
16	M	37	Bisexual	525	4.4	4.6	69.9	AZT, ddC	Virological failure
Mean		30.4		344	3.5	4.5	82		

[a]M, male; F, female; MSM, men having sex with men; VL, HIV-1 viral load in plasma; month 0, time when ART was stopped; month 1, 1 month after ART was stopped. AZT, zidovudine; 3TC, lamivudine; d4T, stavudine; ddI, didanosine; ddC, zalcitabine; ABC, abacavir; EFV, efavirenz; NVP, nevirapine; NFV, nelfinavir; RTV, ritonavir; SQH, saquinavir hard gel capsule; DOV, indinavir; APV, amprenavir; LPV/r, lopinavir + ritonavir.

collected monthly. Measurements of VL (Amplicor HIV-Monitor, Roche Molecular Systems, Inc., NJ) and CD4 and CD8 lymphocyte counts (monoclonal antibodies and flow cytometry) were performed at each blood sampling.

PBMC were separated by centrifugation from 7 ml EDTA-treated blood. PBMC and plasma were stored at −80°C until sequence analysis. The method of sequence analysis was reported previously.[10] Briefly, total RNA was extracted from 100 μl plasma and DNA was extracted from 1×10^6 PBMCs (SMITEST Ex R&D Kit, Japan). The RNA sample was subjected to reverse transcription (RT) followed by nested polymerase chain reaction (PCR) using primers targeting the RT gene and protease (PR) gene, respectively. A DNA sample was also subjected to nested PCR using the same primers for the same targets. The primers covered 1–100 base pairs of PR and 40–240 base pairs of RT. Sequences of primer sets were published elsewhere.[10] Direct sequencing was performed on a 3730 DNA Analyzer (Applied Biosystems). A heterozygous base sequence was identified when the electrogram showed a minor peak at >50% of the major peak. The amino acid sequence was deduced with the GENETYX-WIN version 4.1 (Software Development, Tokyo) and the amino acid substitutions related to drug resistance were estimated from published data.[2] The clade of HIV-1 was determined by the sequences of RT and PR genes.

The reversal period was defined as the time interval between the date of ART interruption and the date of the disappearance of mutations confirmed by direct sequencing. When mutations (all minor mutations, in some patients) did not revert, the reversal period was defined as the date ART stopped to the date most mutations shifted to the wild-type amino acid sequence (for example, see Table 2; protease residues of plasma virus at month 5.9 of patient 2). As all HIV-1s amplified in this study were HIV-1 clade B, we regarded L63P as the polymorphism. The major mutant residues included M41L, A62V, D67N, K70R, L74V, M184V, G190S, L210W, T215F/Y, and K219E/Q of RT mutations and D30N, L33F, M46I, G48V, V82A/F, I84V, and L90M of PR mutations.[2] The follow-up period was the time interval from when ART was interrupted to when the resistance mutations disappeared.

A Kaplan–Meier survival curve was used to estimate the continuous periods of resistance mutations. The Mann–Whitney *U* test was used for group comparisons, the Wilcoxon signed rank test was used for paired comparison of the reversal period, the paired *t*-test was used for changes in CD4 count and HIV-1 viral load, and correlation analysis was used for the relationship between the reversal period and baseline CD4 count or baseline viral load, respectively. StatView version 5 was used for analysis and a p value less than 5% was considered statistically significant.

As shown in Table 1, most patients enrolled in this study had been treated over a long period of time [mean ART period: 82 months (SD, 31.6; range, 46.6–140.8 months)]. The reasons for discontinuation of ART were virologic failure in 10 cases, poor adherence in 4 cases, and side effects in 2 cases. The median follow-up period was 8.9 months (range: 2–25 months) and all patients provided blood samples for testing. None of the patients received any ART during the follow-up period. CD4 counts of 10 patients were more than 200/μl at the time of ART discontinuation. After withdrawal of ART, the CD4 count decreased a mean value of 66/μl 1 month later and continued to decrease until the disappearance of resistant mutations. The VL of 6 patients (patients 7, 9, 10, 11, 13, and 15) who discontinued ART because of side effects or poor adherence ranged from <50 to 650 copies/ml at the time of ART cessation. The VL of these patients rebounded to a mean of 4.2 $\log_{10}$ copies/ml 1 month later (designated as rebounded virus) but showed a plateau level thereafter. The VL of the other 10 patients who discontinued ART for virologic failure was stable after ART cessation.

In all 16 patients, a total of 133 resistance mutation residues with 59 RT and 74 PR were found in plasma and PBMC. The concordance of mutant residues between plasma and PBMC was 96.2% (RT mutations 93.2%, PR mutations 98.6%). All 16 patients possessed RT resistance mutations but 4 of them had no PR mutations (Table 2). In PR, both plasma and PBMC-derived viruses had 26 major resistance and 48 minor resistance residues. In contrast in RT, 52 and 50 major RT residues and 7 and 9 minor RT residues were detected in plasma and PBMC, respectively. The results showed that the resistance mutations could shift to wild type after 1 month or could persist for as long as 22 months after treatment stopped. Interestingly, in 6 patients with viral load rebound, the rebounded viruses in 5 patients (patients 7, 10, 11, 13, and 15) had the same resistant mutations as their predecessor viruses 1 month after ART cessation and then reverted to wild type thereafter. In patient 9, the rebounded virus was a wild-type virus.

As shown in Fig. 1A, after ART interruption, only wild-type virus was detected in 50% of patients at 6.3 months (quartiles, 3.2–20.7 months) and at 9.2 months (quartiles, 5.7–13.8 months) in plasma- and PBMC-derived viruses, respectively. In Fig. 1B, the reversion of 133 resistance mutations is shown by a Kaplan–Meier survival curve. Fifty percent of both PR and RT resistance mutations shifted to wild type in 3.2 months in plasma (quartiles, 1.5–3.7 months for PR, 2–10 months for RT). However, in PBMC, 50% of PR and RT mutations disappeared in 5.7 (quartile, 3.2–6.7 months) and 6.7 (quartile, 3.5–12 months) months, respectively. The reversal period of PR and RT mutations in plasma was 2.5 and 3.5 months, respectively, less than that in PBMC (both $p < 0.05$). Furthermore, the PR mutations shifted to wild type much more rapidly than RT mutations in both plasma and PBMC, although the half life of both mutation residues were the same in plasma (Wilcoxon test $p < 0.05$). In terms of the reversal period of major and minor mutations, there were no difference between them both in the PR and RT regions of plasma- or PBMC-derived viruses. There were no relationships found between the reversal periods of RT and PR mutations and the baseline CD4 cell count, baseline VL, and changes in these two surrogate markers 1 month later (data not shown).

Figure 2 shows how the mutation residues disappeared after ART cessation. We roughly divided the reversal process into two patterns. The first pattern was that resistant mutations persisted for some time and then disappeared abruptly (Fig. 2A). Most PR mutations of plasma viruses, 50% of PR mutations of provirus, and 50% of RT mutations in both types of specimens showed this pattern. The second pattern was that of a gradual decrease of mutations followed by their disappearance or persistence (Fig. 2B). One-third of RT mutations showed this pattern. Overall, all major mutations of RT and PR genes disappeared in all patients after withdrawal of ART. In contrast, the minor mutations did not disappear in some patients.

TABLE 2. RESISTANCE MUTATIONS AND REVERSAL PERIOD IN PLASMA AND PBMC AFTER ART CESSATION

Pt	*Sample*	*Months after ART cessation*	*Reverse transcriptase residues*	*Months after ART cessation*	*Protease residues*
1	Plasma	0	41L, 69D, 118I, 210W, 215Y	0	10I, 30N, 33F, 71T, 84I, 88D, 90M
		3.2	—[a]	3.2	—
	PBMC	0	41L, 69D, 118I, 210W, 215Y	0	10I/L, 30N/D, 33F/L, 71T/A, 84I/V, 88D/N, 90M
		3.2	—	3.2	—
2	Plasma	0	41L, 67N, 69D, 118I, 210W, 215Y	0	10I, 20M, 36I, 48V, 54V, 82A
		15.2[b]	41L, 210W/R	5.9	10F, 36I
	PBMC	0	41L, 67N, 69D, 118I, 210W, 215Y	0	10I, 20M, 36I, 48V, 54V, 82A
		15.2[b]	41L, 118I, 215Y	9	10F, 36I
3	Plasma	0	41L, 44D, 184V, 215Y	0	30N, 71V, 77I, 88D
		7	—	4.6	—
	PBMC	0	41L, 44D, 184V, 215Y	0	30N, 71V, 77I, 88D
		8.6	—	4.6	—
4	Plasma	0	41L, 74V, 184V, 215Y	0	10I, 20I/M, 71V, 73S, 84V, 90M
		2.8	—	4.8	—
	PBMC	0	41L, 184V, 215Y	0	10I/L, 20I, 71V/A, 73S/G, 84V/I, 90M
		4.8	—	4.8	—
5	Plasma	0	41L, 44D, 67N, 210W, 215Y	0	10I, 46I, 71T, 73S, 77I, 82F, 90M
		7.9	—	3.3	10I, 77I
	PBMC	0	41L, 44D, 67N, 184V, 210W, 215Y	0	10I, 46I, 71V, 73S, 77I, 82F, 90M
		12.5	—	6.7	10I, 77I
6	Plasma	0	41L, 74V, 184V, 215Y	0	10I, 46I, 54L, 71V, 77I, 84V, 90M
		6.3	—	1.4	77I
	PBMC	0	41L, 74V/L, V118I, 184V/M, 190G/S, 210W, 215Y	0	10I, 20M/K, 46I, 54L/I, 71V, 77I, 84V, 90M
		11.3	—	3.2	77I
7	Plasma	0	67N, 70R, 184V, 219Q	0	N[c]
		1	67N/D, 70R, 184V/M, 219Q/K		
		3.2	—		
	PBMC	0	67N, 70R, 184V, 219Q	0	N
		9.2	—		
8	Plasma	0	41L, 184V, 215F	0	20R, 36I, 54V, 71V, 82A, 90M
		5.7	—	3.7	—
	PBMC	0	41L, 184V, 215F	0	20R, 36I, 54V, 71V, 82A, 90M
		5.7	—	5.7	20R,
9	Plasma	0	41L, 67N, 70R, 215F, 219E	0	10L/I, 36I, 73S, 77I, 90M
		1	—	1	—
	PBMC	0	67N, 184M/N, 210W, 219E	0	10L/I, 71T/I, 73S, 77I, 90M
		2	—	1	—

10	Plasma	0	41L, 67N, 215F, 219Q	0	10I, 36I, 46I, 53L, 71V, 84V, 90M
		1	41L, 67N, 215F, 219Q		
		8.5[d]	219Q/K	3.7	10I, 36I
	PBMC	0	41L/M, 67N, 70R, 118V/I, 184V/M, 215F, 219Q	0	10I, 36I, 46I, 53L/F, 71V, 84V, 90M
		8.5[d]	67N, 70R, 219Q	7.9	10I, 36I
11	Plasma	0	—	0	N
		1.5	67N, 70R, 219Q		
		24	67N, 69N/D, 219Q		
	PBMC	0	N	0	N
12	Plasma	0	184V, 62V	0	10I, 48V, 71T, 77I, 82A, 90M
		2	—	2.2	71T, 77I
	PBMC	0	184V, 62V	0	10I, 48V, 71T, 77I, 82A, 90M
		2.2	—	5	71T, 77I
13	Plasma	0	67N, 184V	0	10I, 46I, 71V, 77I, 88S
		1	67N, 184V	1	10I, 36M/I, 71V/T
		3.5	—	2.3	10I, 71V/T
	PBMC	0	67N/D, 184V/M	0	10I, 46M/I, 71V/T, 77I
		13.8	—	7.4	10I, 36I/M, 71V/A
14	Plasma	0	184V	0	10I, 20R, 24I, 36I, 53L, 54V, 71T, 82A
		1	—	1	—
	PBMC	0	N	0	10I/L, 20R/K, 24I/L, 36I, 53L/F, 54V, 71V/A, 82V/A
				6.2	—
15	Plasma	0	67N, 70R, 219Q	0	N
		1	67N, 70R		
		20.7	—		
	PBMC	0	67N, 70R, 219Q	0	N
		22.5	67N, 219Q		
16	Plasma	0	67N/D/G, 69A/D, 70R, 219Q	0	N
		19.5	219Q		
	PBMC	0	69A/D, 70R, 219Q	0	N
		19.5	69A/D, 219Q		

[a]—, wild type.
[b]This patient died at this time point with RT mutations detected.
[c]N, no resistance mutations.
[d]New ART was introduced at the time.

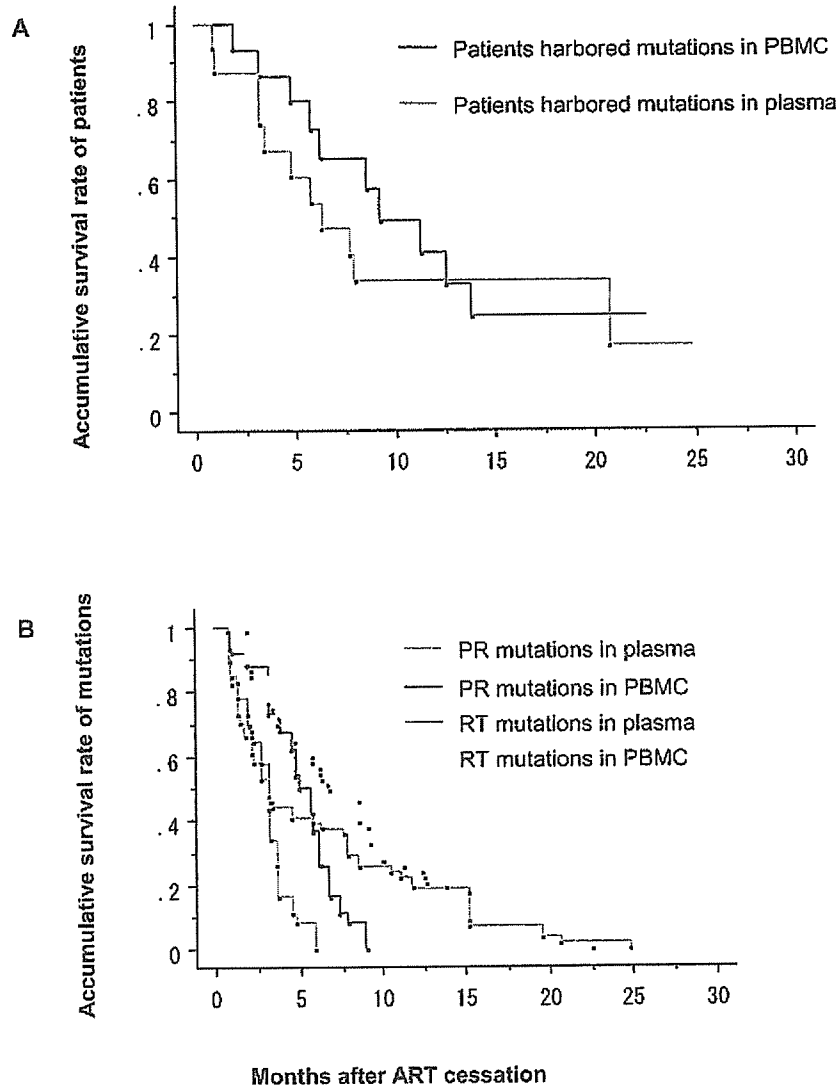

FIG. 1. (A) Kaplan–Meier curves showing percent of 16 patients with drug resistance mutations in plasma or PBMC. (B) Kaplan–Meier curves showing percent of 133 drug resistance mutations (59 RT and 74 PR) in plasma or PBMC. PR, in plasma vs. in PBMC ($p < 0.05$); RT, in plasma vs. in PBMC ($p < 0.05$); PR vs. RT ($p < 0.05$).

We designed the present study with the main objectives of determining the duration of the reversal period from the presence of resistant viruses to wild-type viruses and of elucidating the reversal patterns of plasma- and PBMC-derived viruses after discontinuation of ART. To determine the duration of the reversal period (i.e., from resistant mutations of RT and PR genes of plasma viruses and proviruses to wild type), sequential specimens of plasma and PBMC from patients with resistance mutations were sequenced after ART was interrupted. We found that the PR and RT resistance mutations shifted to wild type much more rapidly in plasma than in PBMC after ART cessation. In 3.2 months after ART stopped, 50% of the resistance mutations in plasma-derived viruses shifted to wild type and 50% of the major mutations of both RT and PR regions were undetected by direct sequencing. This period was similar to that reported by other investigators.[13,14,16–20] However, 50% of the mutations of RT and PR were detected by 6.7 and 5.7 months, respectively, when PBMC samples were used. Accordingly, when the patient develops virologic failure and drug resistance testing is performed using plasma sample after 3.2 months of ART cessation, the results of the test should be interpreted with caution, especially when deciding subsequent ART regimens, because 50% of mutation residues were undetectable by testing. When a resistant virus is not detected by drug-resistant testing, therapy using the same antiretroviral drugs or the same class of agents that reveal cross resistance is usually associated with early drug failure by previously acquired resistant viruses.[23,24] Therefore, like other recommendations,[1,2] drug-resistance testing should be performed soon after ART cessation. However, according to our data, the testing period could be postponed for 2.5 months (from 3.2 to 5.7 months) after ART withdrawal if PBMCs are used instead for plasma. In this regard, PBMC is a suitable candidate specimen for drug-resistance testing during off therapy.

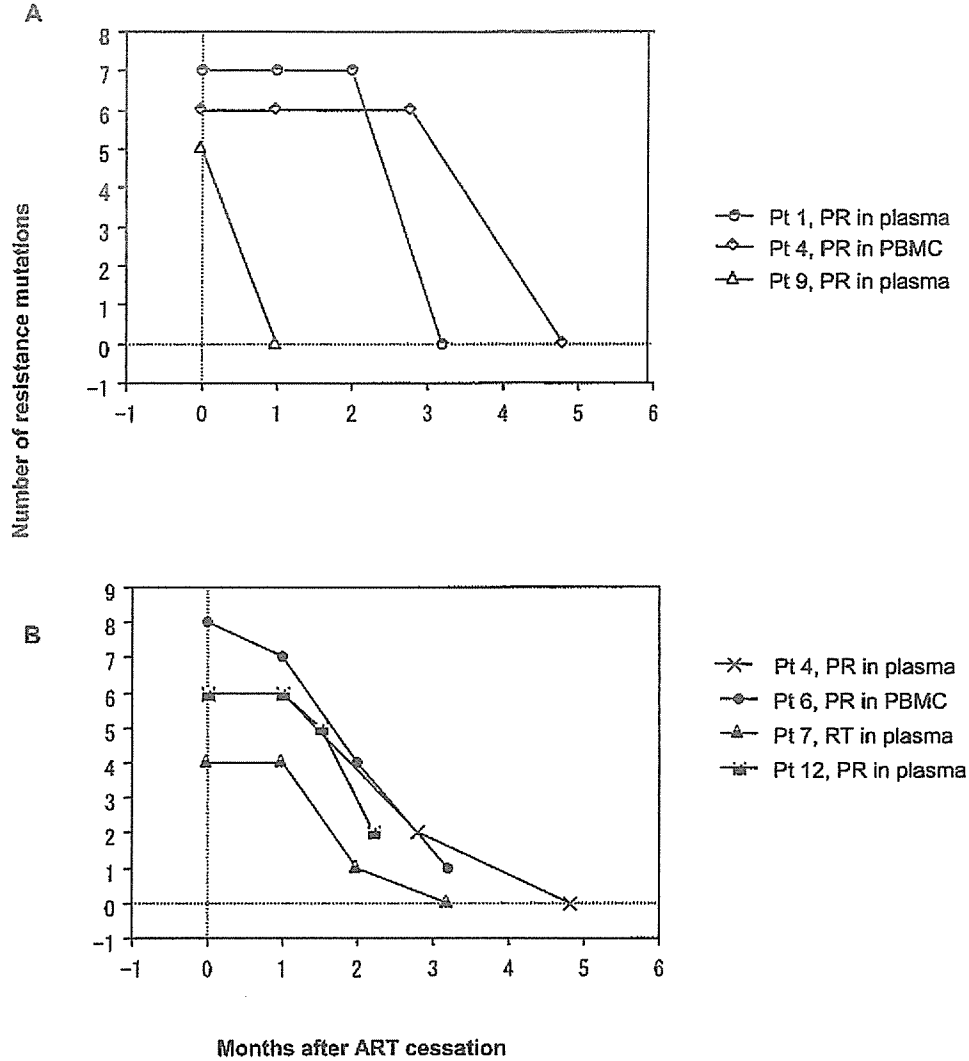

FIG. 2. Two Representative patterns of resistance mutations reverted to wild type after ART cessation. (A) Steep disappearance pattern of resistance mutations; (B) gradual reversal pattern of resistance mutations. RT, reverse transcriptase; PR, protease.

Drug-resistance testing is not advised for patients with VL <1000 copies/ml since amplification of the virus is unreliable.[1,2] However, if ART has to be discontinued because of ART-related toxicities and VL was undetectable at the time of discontinuation, the timing of the test is a practical question. Others report[17] a sharp reduction in the number of mutations at the time of viral load increase in patients during structured treatment interruption. Our results showed that at 1 month after ART cessation, VL dramatically increased from <1000 copies/ml to >4 $\log_{10}$ copies/ml in 6 patients who stopped treatment due to causes other than ART failure. However, the rebounded viruses in 5 of these 6 patients were still resistance mutant but not the wild-type virus. We previously reported that drug resistance mutations emerged gradually when therapy failed.[10] In contrast, the results here showed that nearly 50% of the mutations disappeared abruptly when ART completely stopped. Thus, waiting for several months after ART withdrawal until stabilization of the VL may potentially result in missing important information for selecting the subsequent therapeutic regimen. Therefore, in such situations, drug-resistance testing should be performed after 1 month to obtain a reliable result after ART withdrawal.

We previously studied the emergence of drug resistance during therapy and reported that the appearance of drug resistance in plasma viruses precedes that in proviruses by more than 1 year and recommended the use of plasma samples for drug-resistance testing during therapy.[10] Considering the high concordance of resistance mutations between plasma and PBMC, and the long persistence period of mutations in PBMC, we conclude that when ART stopped, if PBMC could be used as the sample for resistance assay, the test period may be postponed for 3 months.

ACKNOWLEDGMENTS

We are indebted to Drs. S. Ida and K. Tsuchiya for helpful suggestions. We also thank Mrs. F. Negishi and Mrs. Y. Taka-

hashi for sample stock, preparation, and technical support. This study was supported in part by a grant for AIDS Research from the Ministry of Health, Labor, and Welfare of Japan (H15-AIDS-001) and by the Japanese Foundation for AIDS Prevention (X.B.). None of the authors has any conflict of interest.

REFERENCES

1. Department of Health and Human Services: Guidelines for the Use of Antiretroviral Agents in HIV-1-Infected Adults and Adolescents—May 4, 2006. http://aidsinfo.nih.gov/guidelines/.
2. Johnson VA, Brun-Vézinet F, Clotet B, *et al.*: Update of the drug resistance mutations in HIV-1: Fall 2005. International AIDS Society—USA. Top HIV Med 2005;13:125–131.
3. Meynard J-L, Vray M, Morand-Joubert L, *et al.*: Phenotypic or genotypic resistance testing for choosing antiretroviral therapy after treatment failure: A randomized trial. AIDS 2002;16:727–736.
4. Wegner SA, Wallace MR, Aronson NE, *et al.*: Long-term efficacy of routine access to antiretroviral-resistance testing in HIV type 1-infected patients: Results of the clinical efficacy of resistance testing trial. Clin Infect Dis 2004;38:723–730.
5. Tural C, Ruiz L, Holtzer C, *et al.*: Clinical utility of HIV-1 genotyping and expert advice: The Havana trial. AIDS 2002;16:2 09–218.
6. Badri SM, Adeyemi OM, Max BE, Zagorski BM, and Barker DE: How does expert advice impact genotypic resistance testing in clinical practice? Clin Infect Dis 2003;37:708–713.
7. Lorenzi P, Opravil M, Hirschel B, *et al.*: Impact of drug resistance mutations on virologic response to salvage therapy. AIDS 1999; 13:F17–21.
8. Cingolani A, Antinori A, Rizzo MG, *et al.*: Usefulness of monitoring HIV drug resistance and adherence in individuals failing highly active antiretroviral therapy: A randomized study (ARGENTA). AIDS 2002;16:369–379.
9. Sarmati L, Nicastri E, Uccella I, *et al.*: Drug-associated resistance mutations in plasma and peripheral blood mononuclear cells of human immunodeficiency virus type 1-infected patients for whom highly active antiretroviral therapy is failing. J Clin Microbiol 2003;41:1760–1762.
10. Bi X, Gatanaga H, Ida S, *et al.*: Emergence of protease inhibitor resistance-associated mutations in plasma HIV-1 precedes that in proviruses of peripheral blood mononuclear cells by more than a year. J Acquir Immune Defic Syndr 2003;34:1–6.
11. Lawrence J, Mayers DL, Hullsiek KH, *et al.*: Structured treatment interruption in patients with multidrug-resistant human immunodeficiency virus. N Engl J Med 2003;349:837–846.
12. Izopet J, Massip P, Souyris C, *et al.*: Shift in HIV resistance genotype after treatment interruption and short-term antiviral effect following a new salvage regimen. AIDS 2000;14:2247–2255.
13. Miller V, Sabin C, Hertogs K, *et al.*: Virological and immunological effects of treatment interruptions in HIV-1 infected patients with treatment failure. AIDS 2000;14:2857–2867.
14. Deeks SG, Wrin T, Liegler T, *et al.*: Virologic and Immunologic consequences of discontinuing combination antiretroviral-drug therapy in HIV-infected patients with detectable viremia. N Engl J Med 2001;344:472–480.
15. Boucher S, Recordon-Pinson P, Neau D, *et al.*: Clonal analysis of HIV-1 variants in proviral DNA during treatment interruption in patients with multiple therapy failures. J Clin Virol 2005;34(4): 288–294.
16. Pao D, Andrady U, Clarke J, *et al.*: Long-term persistence of primary genotypic resistance after HIV-1 seroconversion. J Acquir Immune Defic Syndr 2004;37:1570–1573.
17. Halfon P, Durant J, Clevenbergh P, *et al.*: Kinetics of disappearance of resistance mutations and reappearance of wild-type during structured treatment interruptions. AIDS 2003;17:1351–1361.
18. Frost SD: Dynamics and evolution of HIV-1 during structured treatment interruptions. AIDS Rev 2002;4:119–127.
19. Verhofstede C, Wanzeele FV, Van Der Gucht B, De Cabooter N, and Plum J: Interruption of reverse transcriptase inhibitors or a switch from reverse transcriptase to protease inhibitors resulted in a fast reappearance of virus strains with a reverse transcriptase inhibitor-sensitive genotype. AIDS 1999;13:2541–2546.
20. Devereux HL, Youle M, Johnson MA, and Loveday C: Rapid decline in detectability of HIV-1 drug resistance mutations after stopping therapy. AIDS 1999;13:F123–F127.
21. Barbour JD, Hecht FM, Wrin T, *et al.*: Persistence of primary drug resistance among recently HIV-1 infected adults. AIDS 2004;18: 1683–1689.
22. Martinez-Picado J, Savara AV, Sutton L, and D'Aquila RT: Replicative fitness of protease inhibitor-resistant mutants of human immunodeficiency virus type 1. J Virol 1999;73:3744–3752.
23. Dykes C, Najjar N, Bosch RJ, *et al.*: Detection of drug-resistance minority variants of HIV-1 during virologic failure of indinavir, lamivudine, and zidovudine. J Infect Dis 2004;189: 1091–1096.
24. Verhofstede C, Noe A, Demecheleer E, *et al.*: Drug-resistant variants that evolve during nonsuppressive therapy persist in HIV-1-infected peripheral blood mononuclear cells after long-term highly active antiretroviral therapy. J Acquir Immune Defic Syndr 2004; 35:473–483.
25. Izopet J, Souyris C, Hance A, *et al.*: Evolution of human immunodeficiency virus type 1 populations after resumption of therapy following treatment interruption and shift in resistance genotype. J Infect Dis 2002;185:1506–1510.

Address reprint requests to:
Shinichi Oka
AIDS Clinical Center, International Medical Center of Japan
1-21-1, Toyama
Shinjuku-ku
Tokyo 162-8655, Japan

E-mail: oka@imcj.hosp.go.jp

Antiviral Chemistry & Chemotherapy 17:167–174

Rapid propagation of low-fitness drug-resistant mutants of human immunodeficiency virus type 1 by a streptococcal metabolite sparsomycin

Kosuke Miyauchi, Jun Komano*, Lay Myint, Yuko Futahashi, Emiko Urano, Zene Matsuda, Tomoko Chiba, Hideka Miura, Wataru Sugiura and Naoki Yamamoto

AIDS Research Center, National Institute of Infectious Diseases, Toyama, Shinjuku, Tokyo, Japan

*Corresponding author: Tel: +81 3 5285 1111; Fax: +81 3 5285 5037; E-mail: ajkomano@nih.go.jp

Here we report that sparsomycin, a streptococcal metabolite, enhances the replication of HIV-1 in multiple human T cell lines at a concentration of 400 nM. In addition to wild-type HIV-1, sparsomycin also accelerated the replication of low-fitness, drug-resistant mutants carrying either D30N or L90M within HIV-1 protease, which are frequently found mutations in HIV-1-infected patients on highly active antiretroviral therapy (HAART). Of particular interest was that replication enhancement appeared profound when HIV-1 such as the L90M-carrying mutant displayed relatively slower replication kinetics. The presence of sparsomycin did not immediately select the fast-replicating HIV-1 mutants in culture. In addition, sparsomycin did not alter the 50% inhibitory concentration (IC_{50}) of antiretroviral drugs directed against HIV-1 including nucleoside reverse transcriptase inhibitors (lamivudine and stavudine), non-nucleoside reverse transcriptase inhibitor (nevirapine) and protease inhibitors (nelfinavir, amprenavir and indinavir). The IC_{50}s of both zidovudine and lopinavir against multidrug resistant HIV-1 in the presence of sparsomycin were similar to those in the absence of sparsomycin. The frameshift reporter assay and Western blot analysis revealed that the replication-boosting effect was partly due to the sparsomycin's ability to increase the –1 frameshift efficiency required to produce the *Gag–Pol* transcript. In conclusion, the use of sparsomycin should be able to facilitate the drug resistance profiling of the clinical isolates and the study on the low-fitness viruses.

Keywords: drug resistant mutants, enhancement of replication, HIV-1, low-fitness mutants, sparsomycin

Introduction

Highly active antiretroviral therapy (HAART) has been successful in controlling the progression of AIDS caused by HIV-1. However, HAART has accelerated the emergence and spread of multidrug-resistant HIV-1. Once drug-resistant HIV-1 occurs in a HIV-1-infected patient, the success rate of HAART drops substantially. Resistance testing has been shown to be valuable to optimize HAART against HIV-1 infection (Hirsch *et al.*, 2000; Rodriguez-Rosado *et al.*, 1999). Profiling drug resistance might be necessary even before the initiation of HAART because of the spread of drug-resistant HIV-1 (Boden *et al.*, 1999; Gehringer *et al.*, 2000; Yerly *et al.*, 1999).

Genotypic and phenotypic resistance testing are the two major ways to determine the drug resistance of clinical HIV-1 isolates. For genotyping, the HIV-1 genome isolated from the infected individuals is sequenced. This HIV-1 genome is than cross-referenced with a database and we are able to predict the drug resistance profile of HIV-1. However, it is impossible to predict the phenotype when we encounter a combination of mutations that has never been documented. This may raise a concern when a new drug is released in the market. Another problem in the genotyping is the presence of genotype-phenotype discordance (Parkin *et al.*, 2003; Sarmati *et al.*, 2002).

Alternatively, for the phenotypic resistance testing, the drug resistance profiles are measured by many biological/virological assay systems (Hertogs *et al.*, 1998; Iga *et al.*, 2002; Jarmy *et al.*, 2001; Kellam & Larder, 1994; Menzo *et al.*, 2000; Walter *et al.*, 1999). Phenotypic resistance testing is powerful because the diagnosis is based on experimental observations. Among the systems, ones that depend on the multi-round HIV-1 replication seemed to provide the best drug resistance data reflecting the *in vivo* condition. However, many drug-resistant mutants have lower replication capabilities than wild-type (wt) HIV-1, which makes the phenotypic resistance testing difficult and time-consuming. In order to overcome these problems, it would be useful to develop a technique to make HIV-1

replicate faster without altering the effectiveness of antiretroviral compounds.

During our search for an inhibitor of HIV-1 replication, we found sparsomycin, a metabolite from *Streptomyces sparsogenes*, which reproducibly enhanced the replication of HIV-1. Therefore, we tested whether sparsomycin merits phenotypic drug resistance profiling studies on low-fitness HIV-1 isolates.

Materials and methods

Cells and viruses

Human embryonic kidney (HEK) 293T cells were maintained in Dulbecco's modified Eagle's medium (Sigma-Aldrich, Tokyo, Japan) supplemented with 10% fetal bovine serum (FBS; Hyclone, Logan, UT, USA), penicillin and streptomycin (Invitrogen, Carlsbad, CA, USA). H9, Jurkat, SupT1 and HPB-Ma cells were maintained in RPMI1640 (Sigma-Aldrich) supplemented with 10% FBS, penicillin and streptomycin. All the cell lines were incubated at 37°C in a humidified 5% CO_2 atmosphere. As previously described, HIV-1 (HXB2) was produced by transfecting proviral DNA into 293T cells and collecting the culture medium 3 days post-transfection (Komano *et al.*, 2004). The replication-incompetent HIV-1 (HXB2 Δ*vpr*, Δ*rev*, Δ*env*, Δ*nef*) was produced by transfecting the proviral DNA carrying renilla luciferase with the *nef* open reading frame into 293T cells, along with the expression plasmid for *env*, *tat*, *rev* and *nef* (pIIIex) as described previously in Komano *et al.* (2004). As previously described, the D30N, L90M, and D25N protease mutants of HIV-1 were generated by the site-directed mutagenesis (Sugiura *et al.*, 2002). The multidrug-resistant HIV-1 DR3577 was a clinical isolate from a patient on HAART in which reverse transciptase carried the following mutations M41L, D67N, K70R, V75M, K101Q, T215F and K219Q and protease carried the following mutations L10I, K20R, M36I, M46I, L63P, A71V, V82T, N88S and L90M. For the generation of replication-incompetent murine leukaemia virus (MLV) vector expressing firefly luciferase, pCMMP luciferase was transfecting into 293T cells along with *gag/pol* and VSV-G expressing plasmids as described previously (Komano *et al.*, 2004).

Chemical compound

Sparsomycin was either purchased from Sigma-Aldrich (cat. S1667) or obtained from Dr Nakajima (Toyama Prefectural University, Toyama, Japan). Sparsomycin was dissolved in 2mM dimethyl sulphoxide and stored at −20°C until use.

Monitoring HIV-1 replication

For HIV-1 infection, 1×10^6 cells were incubated with the culture supernatant containing approximately 10 ng of p24. Alternatively, wt HIV-1, or D30N and L90M mutants were introduced into cells either by electroporation or DEAE-dextran-mediated protocol as previously described (Matsuda *et al.*, 1993; Miyauchi *et al.*, 2005). The culture supernatants were collected everytime the infected cells were split until they ceased to proliferate. The amount of p24 antigen of HIV-1 in the culture supernatants was quantified by using Retro TEK p24 antigen ELISA kit according to the manufacturer's protocol (Zepto Metrix, Buffalo, NY, USA). The signal was detected by Vmax ELISA reader (Molecular Devices, Palo Alto, CA, USA).

Determining 50% inhibitory concentrations (IC_{50})

IC_{50} was calculated by using a reporter cell line, MARBLE, developed by Sugiura *et al.* (personal communication). In brief, a clone of HPB-Ma carrying the long terminal repeat (LTR)-driven firefly luciferase cassette integrated in its genome was infected with HIV-1 and incubated in the presence of varying concentrations of antiretroviral compounds for a week. The cells were then lysed to measure the firefly luciferase activity, which represented the propagation of HIV-1 in culture. The firefly luciferase activity was normalized by constitutively-expressed renilla luciferase activity. The dual luciferase assay was performed according to the manufacturer's protocol (Promega, Madison, WI, USA). Chemiluminescence was detected by Lmax (Molecular Devices).

Reporter assay

The −1 frameshift reporters, pLuc (−1) and pLuc (0), were kindly provided by Dr Brakier-Gingras (Dulude *et al.*, 2002). The renilla luciferase expression vector phRL/CMV was purchased from Promega. pLTR Luc encoded GFP-luciferase under the regulation of HIV-1's LTR promoter (Komano *et al.*, 2004). pLTRΔnefLuc encoded renilla luciferase by substituting *nef* in the proviral context of HXB2 (Komano *et al.*, 2004). Plasmids were transfected into 293T cells by Lipofectamine 2000 plus reagent in accordance with the manufacturers' protocol (Invitrogen). For the detection of luciferase activities, the dual glo luciferase assay was performed at 2–3 days post-transfection or post-infection according to the manufacturers' protocol (Promega). The signal was detected by Vmax ELISA reader (Molecular Devices).

Western blot analysis

COS-7 cells were transfected with Lipofectamine 2000 (Invitrogen) or Fugen6 (Roche, Basel, Switzerland) according to the manufacturer's protocol with proviral DNA encoding the D25N protease mutant. At 48 h post-transfection, cells were washed with PBS and lysed in a buffer containing 4% SDS, 100 mM Tris-HCl (pH 6.8), 12% 2-ME, 20% glycerol and bromophenol blue.

Samples were boiled for 10 min. Protein lysates approximately equivalent to 5×10^4 cells were separated in 5–20% SDS-PAGE (Perfect NT Gel, DRC, Tokyo, Japan), transferred to a polyvinylidene fluoride (PVDF) membrane (Immobilon-P^{SQ}; Millipore, Billerica, MA, USA), and blocked with 5% dried non-fat milk (Yuki-Jirushi, Tokyo, Japan) in PBS. For the primary antibody, we used rabbit anti-*Gag* polyclonal antibody or mouse anti-*Gag* monoclonal antibody. For the secondary antibody, either a biotinylated anti-rabbit antibody or a biotinylated anti-mouse goat antibody (GE Healthcare Bio-Science, Piscataway, NJ, USA) was used. For the tertiary probe, a horseradish peroxidase-conjugated streptoavidin (GE Healthcare Bio-Science) was used. Signals were developed by incubating blots with a chemilumenescent horseradish peroxidase substrate (GE Healthcare Bio-Science) and detected by using Lumi-Imager F1 (Roche).

Results

The structure of sparsomycin, a metabolite from *Streptomyces sparsogenes,* is unique in that it comprises two unusual entities, a monooxodithioacetal moiety and a uracil acrylic acid moiety (Figure 1A). H9 cells were infected with HIV-1 and then maintained in the presence of varying concentrations of sparsomycin. Dimethyl sulphoxide was added in the absence of sparsomycin throughout this study. At 7 days post-infection, a massive syncytial formation was found in the presence of sparsomycin (Figure 1B). The higher the concentration of sparsomycin, the faster p24 accumulated in the culture supernatants (Figure 1C). Similar observations were made in Jurkat, SupT1 (Figures 1D and E), and HPB-Ma cells although the speed of p24 accumulation appeared different among the cell lines. On the other hand, sparsomycin did not show any detectable effect on the cell growth under concentrations of 500 nM.

These results could be due to sparsomycin's ability to either boost HIV-1 replication or select a mutant that replicated substantially faster than the wt HIV-1. To differentiate these possibilities, we recovered the virus-containing culture supernatants from the H9 cell culture at the peak of HIV-1 replication in the presence of 400 nM sparsomycin (asterisk in Figure 1F). Then fresh H9 cells were infected with the recovered virus, the cells were split into two samples and 400 nM of sparsomycin was added to each sample. If sparsomycin selected fast-growing mutants, the replication profiles of HIV-1 should resemble the original sample with sparsomycin (solid circle, Figure 1F) regardless of sparsomycin's presence. However, the replication profile in the presence of sparsomycin shifted leftward (Figure 1G), suggesting that it was unlikely that sparsomycin selected the fast-replicating viral mutants. Therefore, it is likely that sparsomycin boosted HIV-1 replication. Replication-enhancing effects were also seen by using the chemically-synthesized derivatives of sparsomycin (unpublished data; Nakajima *et al.*, 2003). The replication-boosting effect levelled-out at 500 nM, an approximately 20-fold lower concentration than the 50% toxic dose (TD_{50}) of sparsomycin (Ash *et al.*, 1984).

To demonstrate the usefulness of sparsomycin in HIV-1 research, we have examined whether sparsomycin can also boost the replication of drug-resistant low-fitness isolates. The D30N and L90M are common drug-resistant mutations found within HIV-1 protease in HIV-1-infected patients on HAART (Devereux *et al.*, 2001; Kantor *et al.*, 2002; Pellegrin *et al.*, 2002; Sugiura *et al.*, 2002). We introduced proviral DNA carrying the D30N or L90M mutation into H9, Jurkat, and SupT1 cells. HIV-1 replication was than monitored in the presence of 400 nM of sparsomycin. The replication of both viral mutants was substantially enhanced in the presence of sparsomycin in H9 cells (Figures 2A and B). The replication of the L90M-carrying mutant was also enhanced in Jurkat and SupT1 cells (Figures 2C and D). Of note, the replication enhancement appeared profound when HIV-1 displayed relatively slower replication kinetics (for example, the replication of D30N-carrying mutant versus the wt HIV-1 in H9 cells or the replication of HIV-1 in SupT1 versus H9 cells).

Considering the use of sparsomycin in the phenotypic resistance testing, it is critical to know whether sparsomycin affects HIV-1's sensitivity to the antiretroviral drugs. The respective IC_{50} of representative antiretroviral drugs in the absence and the presence of 400 nM sparsomycin were as follows: reverse transcriptase inhibitors; lamivudine, 13.7 and 10.4 nM, and stavudine, 6.3 and 17.0 nM; an non-nucleoside reverse transcriptase inhibitor, nevirapine, 78.2 and 146.4 nM; and protease inhibitors, nelfinavir, 2.8 and 1.0 nM, indinavir, 4.2 and 3.0 nM, and amprenavir, 3.4 and 3.3 nM. Then, we examined whether the presence of sparsomycin affected the IC_{50} of both zidovudine (AZT) and lopinavir (LPV) against a multidrug-resistant HIV-1 isolate, DR3577. The magnitude of both AZT and LPV-resistance of DR3577 was in the order of 2 log (data not shown). The IC_{50}s of AZT in the presence and absence of 400 nM sparsomycin were 14.0 and 36.7 nM, respectively, and for LPV they were 103.1 and 78.9 nM, respectively. These data suggested that the presence of sparsomycin did not significantly influence the IC_{50} of antiretroviral drugs on the replication of both wt and drug-resistant HIV-1.

Finally, we investigated the possible mechanisms that sparsomycin enhanced the replication of HIV-1 and its mutants although the estimated magnitude of enhancement per single replication cycle was small. To do this, we used non-T cells to increase the sensitivity of assays. First, we examined if the early phase of HIV-1's life cycle was

Figure 1. The enhancement of HIV-1 replication by sparsomycin

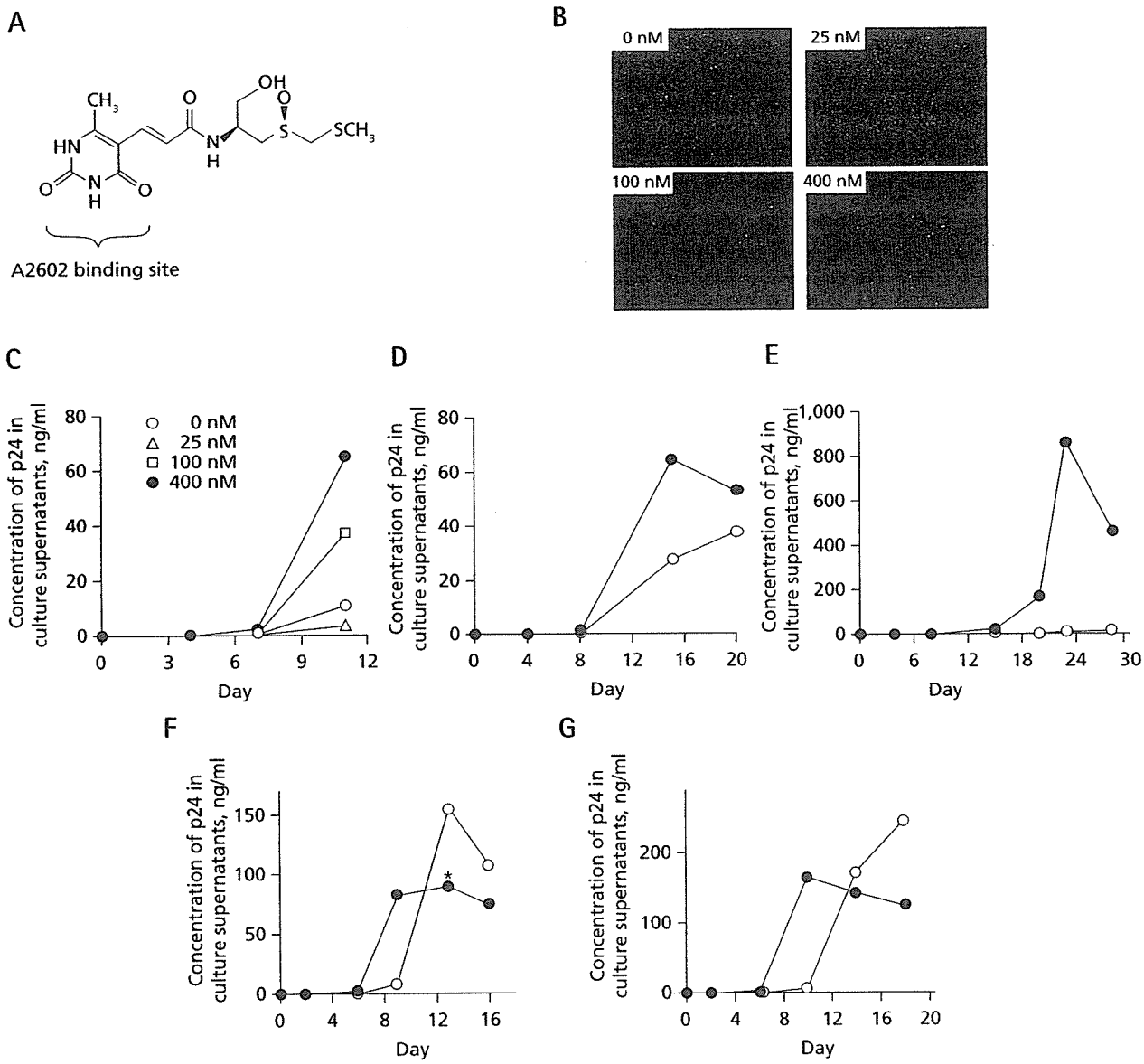

(A) Structure of sparsomycin. The uracil acrylic acid moiety confers the binding capacity to the conserved nucleobase A2602 of the large ribosomal subunit. **(B)** H9 cells infected with HIV-1 were photographed at a week after infection (magnification, ×200). **(C)** The replication profiles of HIV-1 in H9 cells in the presence of varying concentrations of sparsomycin. **(D-G)**. The replication profiles of HIV-1 in Jurkat **(D)**, SupT1 **(E)**, and H9 cells **(F and G)** in the presence of sparsomycin (400 nM, solid circle) or in the absence (open circle; **F and G**). Virus-containing culture supernatant was collected at 13 days post-infection (asterisk, **F**) to infect fresh H9 cells and the replication profiles of HIV-1 were analysed in the presence of sparsomycin (400 nM, solid circle) or in the absence (open circle, **G**).

positively affected by sparsomycin. In the presence of increasing concentrations of sparsomycin, 293 $CD4^+$ T-cells and NP2 CD4 CXCR4 cells were infected with either a replication-deficient HIV-1 vector enveloped with its own *Env* or a VSV-G-psueodotyped MLV vector. Two days post-infection, cells were lysed to measure the luciferase activities representing the efficiency of viral infection. Our results indicate that luciferase activities were not significantly increased at the replication-enhancing dose for both HIV-1 and MLV vectors (Figure 3A). Thus suggesting that the early phase of the retroviral life cycle was not detectably affected by sparsomycin.

Figure 2. Sparsomycin's ability to enhance replication of low-fitness drug resistant HIV-1 mutants

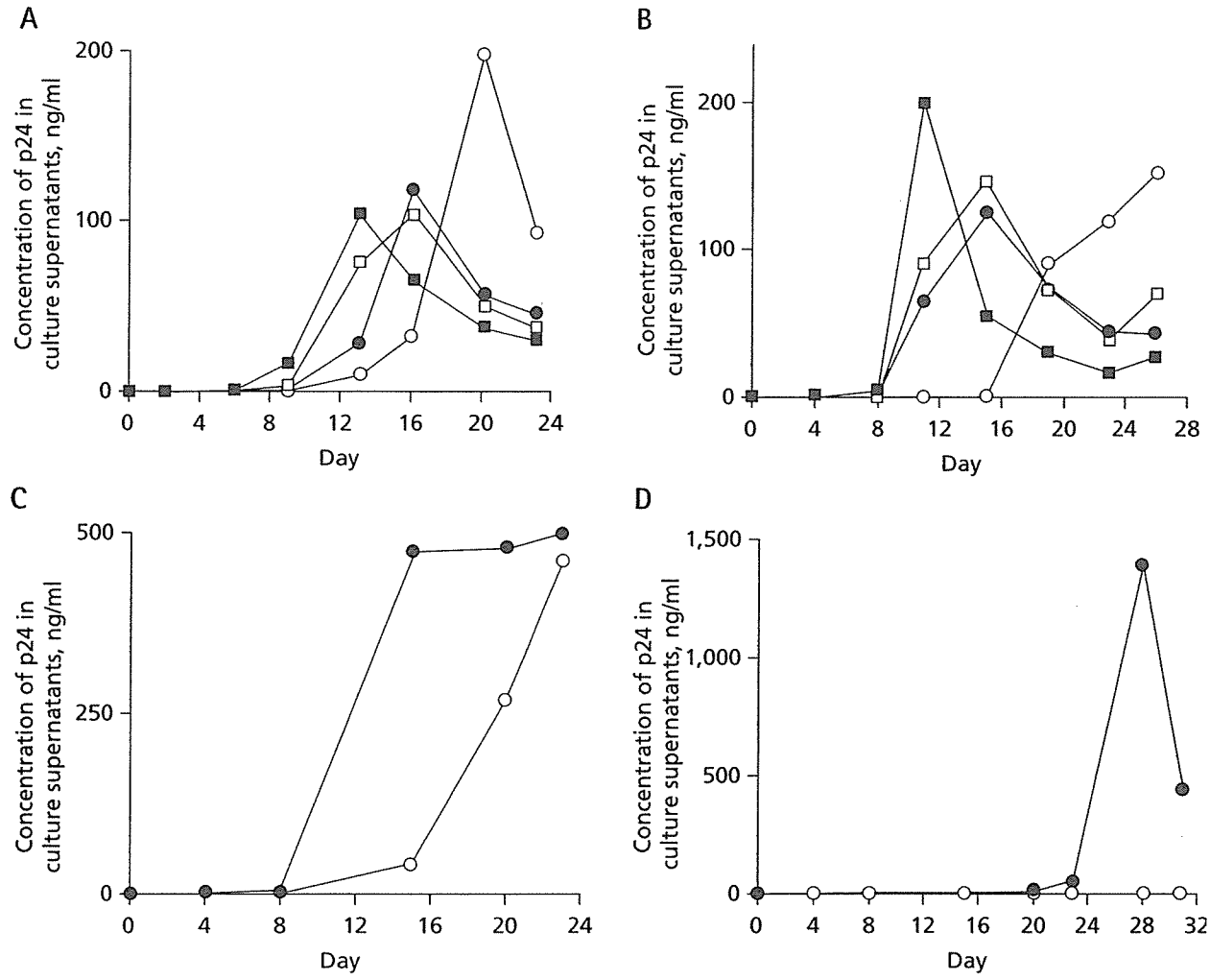

(A and B) The replication kinetics of the D30N-carrying (circle) and L90M-carrying (square) mutants in the presence of sparsomycin (400 nM, solid) or in the absence (open) were investigated twice independently in H9 cells. **(C and D)** The replication kinetics of the L90M-carrying mutant were examined in Jurkat cells **(C)** and SupT1 cells **(D)** in the presence of sparsomycin (400 nM, solid circle) or in the absence (open circle).

Next, we examined the possible active role of sparsomycin in the late phase of HIV-1's life cycle. Sparsomycin has been reported to be a potential enhancer of the −1 frameshift (Dinman *et al.*, 1997). Therefore, we tested whether sparsomycin could positively affect the efficiency of the translational −1 slip at HIV-1's frameshift signal using the reporter assay system established by Dulude *et al.* (2002). The −1 frameshift reporter was created by placing the firefly luciferase in the *pol* frame, pLuc(−1), whereas the control plasmid pLuc(0) has the luciferase in the *gag* frame after the frameshift signal (Figure 3B). In addition, HIV-1's LTR-driven luciferase reporter constructs were tested (pLTR Luc and pLTRΔnefLuc; Figure 3B). We transfected these reporter plasmids into 293T cells along with the renilla luciferase-expressing plasmid phRL/CMV (Promega) to measure the non-specific or toxic effects, if any, of sparsomycin. Cells were incubated in the presence of varying concentrations of sparsomycin for 3 days. Then the dual luciferase assay was performed. The pLuc(−1) behaved differently from the other groups in that the luciferase activities from the pLuc(−1) increased in a dose-dependent fashion. The magnitude of increasement was 2.3-fold at the replication-enhancing dose (Figure 3C). The positive correlation between the relative luciferase activity and the concentration of sparsomycin was statistically significant (r=0.926, P<0.001, n=8, Student's t-test). In contrast, the luciferase activities from the other reporters, even the renilla luciferase plasmid

co-transfected with the pLuc(-1) vector, remained unchanged (Figure 3C). These data suggested that sparsomycin positively affected the efficiency of HIV-1's −1 frameshift. It also suggested that sparsomycin did not enhance transcription from the viral promoter or the translation of proteins driven by the LTR promoter to enhance HIV-1 replication.

If the efficiency of −1 frameshift was increased, we would expect that the *Gag–Pol* to *Gag* ratio to increase. To test this, we transfected COS-7 cells with the HIV-1's proviral DNA carrying the D25N mutation in protease that produced catalytically inactive protease to increase the sensitivity of detecting *Gag–Pol* (Xie *et al.*, 1999). When sparsomycin was added, the intensities of *Gag–Pol* gradually increased in relation to the reporter assay. The *Gag–Pol* to *Gag* ratio reached 1.3-fold at 400 nM sparsomycin when normalized with results produced in the absence of sparsomycin (Figure 3D). The average and standard deviation of the *Gag–Pol* to *Gag* ratio from four independent experiments were 1.29 ±0.14 at the replication enhancing concentration of sparsomycin (1.29-, 1.48-, 1.16-, and 1.24-fold increase). Similar results were obtained by using

Figure 3. The possible mechanism of HIV-1 replication enhancement by sparsomycin

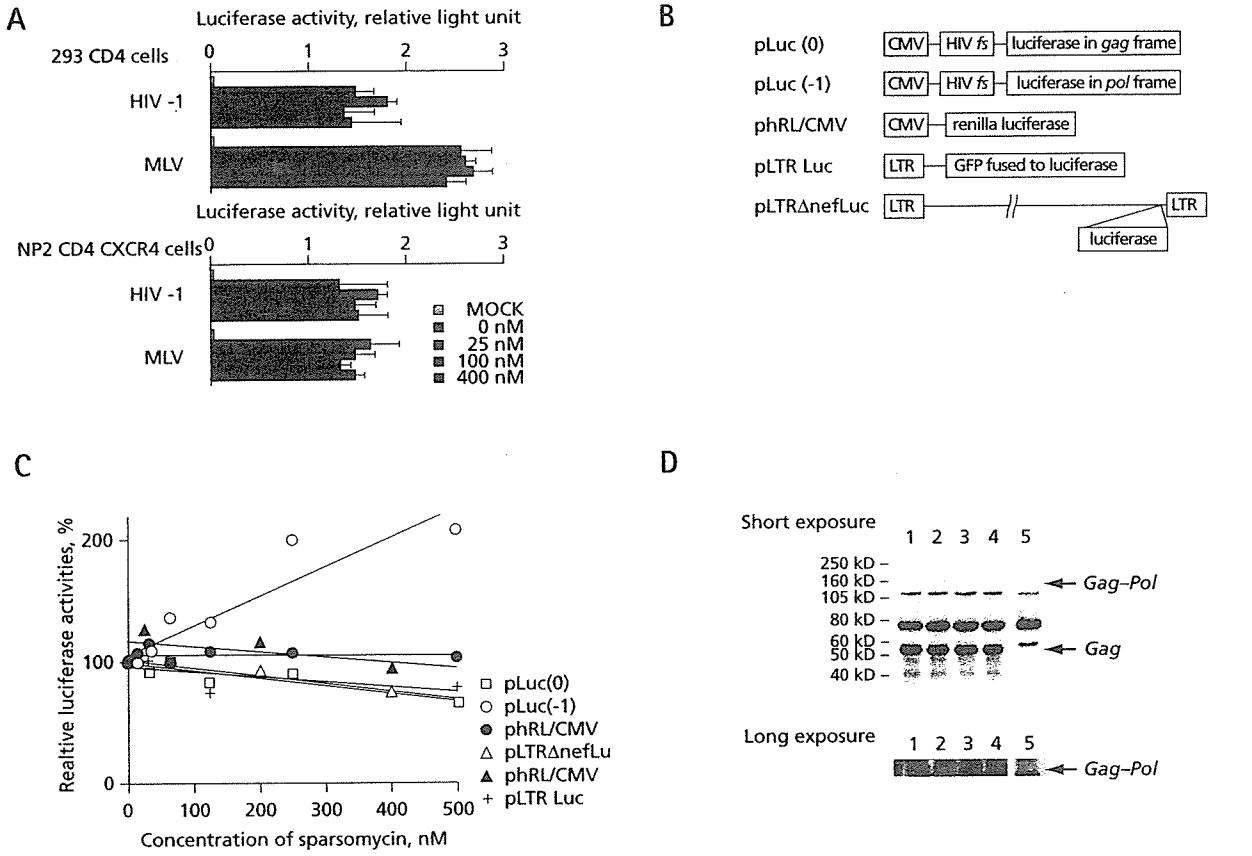

(A) The single round infection efficiencies of HIV-1 and murine lukaemia virus (MLV) vectors measured by the virally-encoded luciferase activities in 293 CD4$^+$ T-cells and NP2 CD4 CXCR4 cells in the presence of varying concentrations of sparsomycin. **(B)** The schematic drawing of constructs used in the reporter assay. The HIV-1's frameshift signal (*fs*) was placed between the CMV promoter and the luciferase. The luciferase was placed in either the *gag* frame (pLuc(0)) or the *pol* frame (pLuc(-1)). The renilla luciferase expression vector phRL/CMV was used in parallel. The pLTR Luc encodes the GFP-luciferase driven by HIV-1's LTR promoter. The pLTRΔnefLuc has the renilla luciferase substituting *nef* in the proviral context of HXB2. **(C)** The luciferase activities from the above reporter constructs without sparsomycin were set as 100% and the relative luciferase activities in the presence of sparsomycin were shown. The renilla luciferase activities from phRL/CMV were shown for the pLuc(-1) (solid circle) and pLTRΔnefLuc (solid triangle) transfections in particular. The pLuc(-1) behaved differently from the other groups and the positive correlation between the relative luciferase activity and the concentration of sparsomycin was statistically significant (r=0.926, P<0.001, n=8, Student's t-test). The SD was within 10% from the avgerage. Shown are the representative data from two independent experiments. **(D)** Western blot analysis to measure the *Gag–Pol* and *Gag* ratio. Cell extracts were separated in the SDS-polyacrylamide gel and immunoblotted by using the rabbit polyclonal antibodies raised against p24. (lane 1, 0 nM; lane 2, 20 nM; lane 3, 200 nM; lane 4, 400 nM; lane 5, MOCK). The lower panel shows the *Gag–Pol* signal obtained from the long exposure of the same blot.

two different antibodies recognizing *Gag*. We were unable to detect a significant increase in the *Env:Gag* ratio (unpublished data), suggesting that the sparsomycin's effect on *Gag–Pol:Gag* ratio was specific. These data suggested that the translational efficiencies of viral proteins were not equally enhanced by sparsomycin. Altogether, it was strongly suggested that the sparsomycin's replication-boosting effect on HIV-1 was partly due to the enhancement of the –1 frameshift efficiency.

Discussion

In the present study, we have demonstrated that sparsomycin is an enhancer of HIV-1 replication in many human T cell lines at concentrations between 400–500nM. Our preliminary observation suggested that HIV-1 replication was also enhanced in primary peripheral blood monocyte culture (data not shown). Sparsomycin should be able to accelerate the study on the low-fitness HIV-1 such as drug-resistant mutants. As sparsomycin did not alter the IC_{50} of multiple antiretroviral drugs on both wt and drug-resistant HIV-1, its usage should be able to facilitate the phenotypic resistance testing of clinical isolates and as a result, benefit HIV-1-infected patients. Our observation raised an immediate concern as to whether sparsomycin-producing Streptomyces species caused an opportunistic infection in humans, which influenced AIDS progression. However, we did not find any reports suggesting so.

Sparsomycin and puromycin are the only antibiotics that can inhibit protein synthesis in bacterial, archaeal and eukaryotic cells (Ottenheijm *et al.*, 1986; Porse *et al.*, 1999). Sparsomycin has the ability to enhance the –1 frameshift in mammalian cells as well as *S. cervisiae* (Dinman *et al.*, 1997). The proposed molecular mechanism behind this ability was either through a higher affinity of the donor stem for the ribosome and slowing down the rate of the peptidyl transfer reaction, or a change in the steric alignment between donor and acceptor tRNA stems resulting in decreased peptidyl-transfer rates. Conversely, puromycin is not known to enhance the –1 frameshift in mammalian cells. At sub-toxic concentrations, puromycin was unable to enhance the HIV-1 replication (unpublished data). These data, along with the data provided in this paper, implied that the sparsomycin's unique ability to enhance the –1 frameshift might play a role in boosting the HIV-1 replication.

The maintenance of the –1 frameshift efficiency at the optimal range is critical for HIV-1 to replicate (Jacks *et al.*, 1988). Therefore, limiting *Gag–Pol* production should lead to an inhibition of viral replication because *pol* encodes enzymes essential for viral replication (Levin *et al.*, 1993). In contrast, it was also reported that increasing the *Gag–Pol* to *Gag* ratio by twofold resulted in a reduction of viral replication (Hung *et al.*, 1998; Shehu-Xhilaga *et al.*, 2001). Thus, a modest alteration of the –1 frameshift efficiency should markedly affect the replication capacity of HIV-1. Our data indicated that sparsomycin increased the efficiency of –1 frameshift by 1.3-fold, which produces a better replication capacity for HIV-1. As a result, we hypothesize that HIV-1 has a 'suboptimal' –1 frameshift efficiency. In theory, the 1.3-fold difference per one replication cycle becomes approximately 10-fold after 10 rounds of viral replication cycle because the effect accumulates exponentially. The difference should become larger when HIV-1 replicates with the slower kinetics and the replication profile is monitored over a longer time course. In fact, our experimental data were in good agreement with the above estimation. In nature, HIV-1 does not accumulate mutations within the frameshift signal to achieve the higher frameshift efficiencies. This implies that there are multiple and complex regulatory mechanisms that keep the efficiency of the –1 frameshift at suboptimum. Under these conditions, the best efficiency of HIV-1 survival in the host might be achieved. Altogether, one of the possible mechanisms that sparsomycin boosted the HIV-1 replication could be the enhancement of the –1 frameshift efficiency.

Acknowledgements

We thank Drs Hironori Sato and Tsutomu Murakami for critical reading of the manuscript. This work was partly supported by both the Japan Health Science Foundation and the grant from Japanese Ministry of Health, Labor, and Welfare.

References

Ash RJ, Fite LD, Beight DW & Flynn GA (1984) Importance of the hydrophobic sulfoxide substituent on nontoxic analogs of sparsomycin. *Antimicrobial Agents and Chemotherapy* **25**:443–445.

Boden D, Hurley A, Zhang L, Cao Y, Guo Y, Jones E, Tsay J, Ip J, Farthing C, Limoli K, Parkin N & Markowitz M (1999) HIV-1 drug resistance in newly infected individuals. *Journal of the American Medical Association* **282**:1135–1141.

Devereux HL, Emery VC, Johnson MA & Loveday C (2001) Replicative fitness *in vivo* of HIV-1 variants with multiple drug resistance-associated mutations. *Journal of Medical Virology* **65**:218–224.

Dinman JD, Ruiz-Echevarria MJ, Czaplinski K & Peltz SW (1997) Peptidyl-transferase inhibitors have antiviral properties by altering programmed -1 ribosomal frameshifting efficiencies: development of model systems. *Proceedings of the National Academy of Sciences of the United States of America* **94**:6606–6611.

Dulude D, Baril M & Brakier-Gingras L (2002) Characterization of the frameshift stimulatory signal controlling a programmed -1 ribosomal frameshift in the human immunodeficiency virus type 1. *Nucleic Acids Research* **30**:5094–5102.

Gehringer H, Bogner JR, Goebel FD, Nitschko H & von der Helm K (2000) Sequence analysis of the HIV-1 protease coding region of 18 HIV-1-infected patients prior to HAART and possible implications on HAART. *Journal of Clinical Virology* **17**:137–141.

Hertogs K, de Bethune MP, Miller V, Ivens T, Schel P, Van Cauwenberge A, Van Den Eynde C, Van Gerwen V, Azijn H, Van Houtte M, Peeters F, Staszewski S, Conant M, Bloor S, Kemp S, Larder B & Pauwels R (1998) A rapid method for simultaneous detection of phenotypic resistance to inhibitors of protease and reverse transcriptase in recombinant human immunodeficiency virus type 1 isolates from patients treated with antiretroviral drugs. *Antimicrobial Agents and Chemotherapy* **42**:269–276.

Hirsch, MS, Brun-Vezinet F, D'Aquila RT, Hammer SM, Johnson, VA, Kuritzkes DR, Loveday C, Mellors JW, Clotet B, Conway B, Demeter LM, Vella S, Jacobsen DM & Richman DD (2000) Antiretroviral drug resistance testing in adult HIV-1 infection: recommendations of an International AIDS Society-USA Panel. *Journal of the American Medical Association* **283**:2417–2426.

Hung M, Patel P, Davis S & Green SR (1998) Importance of ribosomal frameshifting for human immunodeficiency virus type 1 particle assembly and replication. *Journal of Virology* **72**:4819-4824.

Iga M, Matsuda Z, Okayama A, Sugiura W, Hashida S, Morishita K, Nagai Y & Tsubouchi H (2002) Rapid phenotypic assay for human immunodeficiency virus type 1 protease using *in vitro* translation. *Journal of Virological Methods* **106**:25–37.

Jacks T, Power MD, Masiarz FR, Luciw PA, Barr PJ & Varmus HE. (1988) Characterization of ribosomal frameshifting in HIV-1 gag-pol expression. *Nature* **331**:280–283.

Jarmy G, Heinkelein M, Weissbrich B, Jassoy C & Rethwilm A (2001) Phenotypic analysis of the sensitivity of HIV-1 to inhibitors of the reverse transcriptase, protease, and integrase using a self-inactivating virus vector system. *Journal of Medical Virology* **64**:223–231.

Kantor R, Fessel WJ, Zolopa AR, Israelski D, Shulman N, Montoya JG, Harbour M, Schapiro JM & Shafer RW (2002) Evolution of primary protease inhibitor resistance mutations during protease inhibitor salvage therapy. *Antimicrobial Agents and Chemotherapy* **46**:1086–1092.

Kellam P & Larder BA (1994) Recombinant virus assay: a rapid, phenotypic assay for assessment of drug susceptibility of human immunodeficiency virus type 1 isolates. *Antimicrobial Agents and Chemotherapy* **38**:23–30.

Komano J, Miyauchi K, Matsuda Z & Yamamoto N (2004). Inhibiting the Arp2/3 Complex limits infection of both intracellular mature vaccinia virus and primate lentiviruses. *Mol Biol Cell* **15**:5197–5207.

Levin JG, Hatfield DL, Oroszlan S & Rein A (1993) Mechanisms of translational suppression used in the biosynthesis of reverse transcriptase. In *Reverse transcriptase*, pp. 5–31. Edited by AM Skalka & SP Goff. New York: Cold Spring Harbor Laboratory Press.

Matsuda Z, Yu X, Yu QC, Lee TH & Essex M (1993) A virion-specific inhibitory molecule with therapeutic potential for human immunodeficiency virus type 1. *Proceedings of the National Academy of Sciences of the United States of America* **90**:3544–3548.

Menzo S, Rusconi S, Monachetti A, Colombo MC, Violin M, Bagnarelli P, Varaldo PE, Moroni M, Galli M, Balotta C & Clementi M (2000) Quantitative evaluation of the recombinant HIV-1 phenotype to protease inhibitors by a single-step strategy. *AIDS* **14**:1101–1110.

Miyauchi K, Komano J, Yokomaku Y, Sugiura W, Yamamoto N & Matsuda, Z (2005) Role of the specific amino acid sequence of the membrane-spanning domain of human immunodeficiency virus type 1 in membrane fusion. *Journal of Virology* **79**:4720–4729.

Nakajima N, Enomoto T, Watanabe T, Matsuura N & Ubukata M. (2003) Synthesis and activity of pyrimidinylpropenamide antibiotics: the alkyl analogues of sparsomycin. *Bioscience, Biotechnology, and Biochemistry* **67**:2556–2566.

Ottenheijm HC, van den Broek LA, Ballesta JP & Zylicz Z (1986) Chemical and biological aspects of sparsomycin, an antibiotic from Streptomyces. *Progress in Medicinal Chemistry* **23**:219–268.

Parkin NT, Chappey C & Petropoulos CJ (2003) Improving lopinavir genotype algorithm through phenotype correlations: novel mutation patterns and amprenavir cross-resistance. *AIDS* **17**:955–961.

Pellegrin I, Breilh D, Montestruc F, Caumont A, Garrigue I, Morlat P, Le Camus C, Saux MC, Fleury HJ & Pellegrin JL (2002) Virologic response to nelfinavir-based regimens: pharmacokinetics and drug resistance mutations (VIRAPHAR study). *AIDS* **16**:1331–1340.

Porse BT, Kirillov SV, Awayez MJ, Ottenheijm HC & Garrett RA (1999) Direct crosslinking of the antitumor antibiotic sparsomycin, and its derivatives, to A2602 in the peptidyl transferase center of 23S-like rRNA within ribosome-tRNA complexes. *Proceedings of the National Academy of Sciences of the United States of America* **96**:9003–9008.

Rodriguez-Rosado R, Briones C & Soriano V (1999) Introduction of HIV drug-resistance testing in clinical practice. *AIDS* **13**:1007–1014.

Sarmati L, Nicastri E, Parisi SG, d'Ettorre G, Mancino G, Narciso P, Vullo V & Andreoni M (2002) Discordance between genotypic and phenotypic drug resistance profiles in human immunodeficiency virus type 1 strains isolated from peripheral blood mononuclear cells. *Journal of Clinical Microbiology* **40**:335–340.

Shehu-Xhilaga M, Crowe SM & Mak J (2001) Maintenance of the Gag/Gag-Pol ratio is important for human immunodeficiency virus type 1 RNA dimerization and viral infectivity. *Journal of Virology* **75**:1834–1841.

Sugiura W, Matsuda Z, Yokomaku Y, Hertogs K, Larder B, Oishi T, Okano A, Shiino T, Tatsumi M, Matsuda M, Abumi H, Takata N, Shirahata S, Yamada K, Yoshikura H & Nagai Y (2002) Interference between D30N and L90M in selection and development of protease inhibitor-resistant human immunodeficiency virus type 1. *Antimicrobial Agents and Chemotherapy* **46**:708–715.

Walter H, Schmidt B, Korn K, Vandamme AM, Harrer T & Uberla K. (1999). Rapid, phenotypic HIV-1 drug sensitivity assay for protease and reverse transcriptase inhibitors. *Journal of Clinical Virology* **13**:71–80.

Xie D, Gulnik S, Gustchina E, Yu B, Shao W, Qoronfleh W, Nathan A & Erickson JW (1999) Drug resistance mutations can effect dimer stability of HIV-1 protease at neutral pH. *Protein Science* **8**:1702–1707.

Yerly S, Kaiser L, Race E, Bru JP, Clavel F & Perrin L (1999) Transmission of antiretroviral-drug-resistant HIV-1 variants. *Lancet* **354**:729–733.

Received 5 December 2005, accepted 23 March 2006

THE JOURNAL OF IMMUNOLOGY

CUTTING EDGE

Cutting Edge: Uniqueness of Lymphoid Chemokine Requirement for the Initiation and Maturation of Nasopharynx-Associated Lymphoid Tissue Organogenesis[1]

Satoshi Fukuyama, Takahiro Nagatake,* Dong-Young Kim,* Kaoru Takamura,* Eun Jeong Park,* Tsuneyasu Kaisho,† Norimitsu Tanaka,‡ Yuichi Kurono,‡ and Hiroshi Kiyono[2]**

CD3$^-$CD4$^+$CD45$^+$ inducer cells are required for the initiation of mucosa-associated organogenesis of both nasopharynx-associated lymphoid tissues (NALT) and Peyer's patches (PP) in the aerodigestive tract. CXCL13$^{-/-}$ mice and mice carrying the paucity of lymph node T cell* (plt) *mutation and lacking expression of CCL19 and CCL21 accumulate CD3$^-$CD4$^+$CD45$^+$ cells at the site of NALT but not of PP genesis. Although NALT was observed to develop in adult CXCL13$^{-/-}$ and* plt/plt *mice, the formation of germinal centers in CXCL13$^{-/-}$ mice was affected, and their population of B cells was much lower than in the NALT of CXCL13$^{+/-}$ mice. Similarly, fewer T cells were observed in the NALT of* plt/plt *mice than in control mice. These findings indicate that the initiation of NALT organogenesis is independent of CXCL13, CCL19, and CCL21. However, the expression of these lymphoid chemokines is essential for the maturation of NALT microarchitecture. The Journal of Immunology,* 2006, 177: 4276–4280.

Nasopharynx-associated lymphoid tissue (NALT)[3] plays a pivotal role in the initiation of Ag-specific immune responses at both systemic and mucosal sites (1). Thus, NALT acts as an important inductive site for the generation of Ag-specific IgA-committed B cells (1). In addition, although NALT possesses a predominance of naive Th0 CD4$^+$ cells, the Ag-specific Th1 and/or Th2 immune responses can be induced in NALT through intranasal administration of Ags and mucosal adjuvants (e.g., cholera toxin) (1). Thus, NALT is thought to be a key secondary lymphoid structure for the upper respiratory tract.

The lymphotoxin (LT)βR signaling pathway is essential for the organogenesis of secondary lymphoid tissues, including peripheral lymph nodes (LN) and Peyer's patches (PP) (2). However, previous reports by our and other groups (3, 4) have demonstrated that NALT organogenesis, unlike that of other secondary lymphoid tissues, can occur independently of the LTβR signaling pathway. Inducer cells with phenotypes of CD3$^-$, CD4$^+$, and CD45$^+$ are required for the initiation of the organogenesis of NALT, PP, and LN (1–3). Lymphoid chemokines, including CXCL13, CCL19, and CCL21, have been shown to be important for the recruitment of CD3$^-$CD4$^+$CD45$^+$ cells to the PP anlagen (5, 6). Not surprisingly then, CXCR5$^{-/-}$ mice and CXCL13$^{-/-}$ mice lack PP and several types of LN such as inguinal and iliac LN (7). Although PP and LN are developed in mice carrying the paucity of LN T cell (*plt*) mutation, which are known not to produce CCR7 ligands, CCL19 and CCL21, a study using double mutants of CXCL13$^{-/-}$ and *plt/plt* mice revealed that CCL19, CCL21, and CXCL13 were cooperatively involved in the development of secondary lymphoid organs (7). However, little is known about the involvement of these lymphoid chemokines for the recruitment of CD3$^-$CD4$^+$CD45$^+$ cells to sites of NALT development.

To better understand the varying roles of lymphoid chemokines in the development of NALT and the maintenance of its architecture, we investigated the unique characteristics of NALT development using CXCL13$^{-/-}$ mice and *plt/plt* mice. Our results provide the first evidence that the initiation of NALT organogenesis is independent of lymphoid chemokines,

*Division of Mucosal Immunology, Department of Microbiology and Immunology, The Institute of Medical Science, The University of Tokyo, Tokyo, Japan; †RIKEN Research Center for Allergy and Immunology, Yokohama, Japan; and ‡Department of Otolaryngology, Head and Neck Surgery, Kagoshima University Graduate School of Medical and Dental Sciences, Kagoshima, Japan

Received for publication May 8, 2006. Accepted for publication August 1, 2006.

The costs of publication of this article were defrayed in part by the payment of page charges. This article must therefore be hereby marked *advertisement* in accordance with 18 U.S.C. Section 1734 solely to indicate this fact.

[1] This work was supported by the Core Research for Evolutional Science and Technology Program, from Japan Science and Technology Corporation, and a Grant-in-Aid from the Ministry of Education, Science, Sports, and Culture and the Ministry of Health and Welfare of Japan. S.F. was supported by research fellowships from the Japan Society for the Promotion of Science for Young Scientists. D.-Y.K. was supported by research fellowships from the Japan Society for the Promotion of Science for Foreign Researchers.

[2] Address correspondence and reprint requests to Dr. Hiroshi Kiyono, Division of Mucosal Immunology, Department of Microbiology and Immunology, The Institute of Medical Science, The University of Tokyo, 4-6-1 Shirokanedai, Minato-ku, Tokyo 108-8639, Japan. E-mail address: kiyono@ims.u-tokyo.ac.jp

[3] Abbreviations used in this paper: NALT, nasopharynx-associated lymphoid tissue; PP, Peyer's patch; LT, lymphotoxin; LN, lymph node; E17, 17-day-old embryo; LDM, laser microdissection; FDC, follicular dendritic cell; PNA, peanut agglutinin; NALTi, NALT inducer cell; PPi, PP inducer cell; MLN, mesenteric LN.

0022-1767/06/$02.00

including CXCL13, CCL19, and CCL21. Lymphoid chemokines have been shown to play an important role in the maturation of the microarchitecture of secondary lymphoid organs (8, 9), and our current findings show that these same chemokines are essential for NALT microarchitecture formation as well.

Materials and Methods

Mice

BALB/c and C57BL/6 mice were purchased from Japan SLC. The procedure for generating CXCL13$^{-/-}$ mice on a C57BL/6 background was reported previously (10). *Plt/plt* mice with a BALB/c background were provided from Drs. H. Nakano and T. Kakiuchi (Department of Immunology, Toho University School of Medicine, Tokyo, Japan) (11). CXCL13$^{-/-}$*plt/plt* mice were generated by intercrossing CXCL13$^{-/-}$ mice with *plt/plt* mice. PCR primers D4Mit237 (sense, 5′-TTCAAACTCATGAGTCTATGGGG-3′; antisense, 5′-ATATACACGTAGACTCGCACGC-3′) were used to determine the genome type of *plt/plt* and *plt/+* or +/+ (11).

Cell analysis and isolation by flow cytometry

Cells were isolated from the nasal tissues and intestines and then stained with the appropriate fluorescence-conjugated anti-CD3ε (145-2C11; BD Pharmingen), anti-CD45 (30-F11; BD Pharmingen), anti-CD4 (L3T4; BD Pharmingen), anti-B220 (RA3-6B2; BD Pharmingen), anti-CD11c (HL3; BD Pharmingen), anti-CXCR5 (2G8; BD Pharmingen), and/or anti-CCR7 (4B12; eBioscience) (3). Cells were then analyzed using a FACSCalibur flow cytometer (BD Biosciences), and data analysis was performed with CellQuest software (BD Biosciences). For the purification of CD3$^-$CD4$^+$CD45$^+$ cells from infant nasal tissues (10-day-old) and embryonic intestines (17-day-old embryos (E17)), we used an AutoMACS (Miltenyi Biotec) combined with a FACSAria cell sorter (BD Biosciences), as described previously (3).

Isolation of NALT anlagen for RT-PCR

Following the manufacturer's recommendations, we obtained RNA from NALT anlagen by using the laser microdissection (LMD) system (Leica Microsystems). Unfixed nasal tissues isolated from newborn, 7-day-old, 14-day-old, and 6-wk-old mice were frozen in liquid nitrogen. Samples were sectioned into 8-μm thicknesses and immediately fixed in 75% ethanol/diethylpyrocarbonate-treated water for 30 s. Sections were counterstained with toluidine blue (Wako Pure Chemical) for 30 s. After the dehydration with ethanol and xylene, the sections were dissected with a LMD system (Leica Microsystems). The site of NALT formation was captured from each tissue and lysed in TRIzol (Invitrogen Life Technologies) for quantitative RT-PCR using the LightCycler system (Roche Diagnostics) (12).

Primers and hybrid probes for real-time RT-PCR

The primers and hybrid probes used for PCR were as follows: the oligonucleotide primers specific for CXCR5 (sense, 5′-TTCTCCACCCAATGTACC-3′; antisense, 5′-AACCTCTGTCGTCATTCTC-3′), CXCR5 detection FITC-labeled probe (5′-ATTCTACGCACCAATGGGGAAGGAAGC CAACT-3′), and LightCycler Red 640-labeled hybrid probe (5′-GCCTGGG GAAAGCAAGATAGCAAAGTGGTCCTA-3′); the oligonucleotide primers specific for CCR7 (sense, 5′-ATGCTGGCTATGAGTTTC-3′; antisense, 5′-GCTGCTATTGGTGATGTT-3′), CCR7 detection FITC-labeled probe (5′-ATGATCACCTTGATGGCCTTGTTCCGCTCAAAG-3′), and LightCycler Red 640-labeled hybrid probe (5′-TGCGTGCCTGGAGCAAGG TACGGATGATAATGA-3′); the oligonucleotide primers specific for CXCL13 (sense, 5′-GAACAGGCATTTAGTGACAAC-3′; antisense, 5′-TTTTGGAAGCCTGCGTTTT-3′), CXCL13 detection FITC-labeled probe (5′-AATGTGAACTTGTAGCTCGTACTAACAAGAGG-3′), and LightCycler Red 640-labeled hybrid probe (5′-TTGCGAGATGGACT TCAGTTATTTTGCACC-3′); the oligonucleotide primers specific for CCL19 (sense, 5′-GCCAAGAACAAAGGCAACA-3′, antisense, 5′-CA CACTCACATCGACTCTCTA-3′), CCL19 detection FITC-labeled probe (5′-TGGCCCAGGAAACCAAGGACCA-3′), and LightCycler Red 640-labeled hybrid probe (5′-AAGAGAGGACCAGGCCTCCT-3′); the oligonucleotide primers specific for CCL21a (sense, 5′-ACAGACACAGCCCTCAA-3′; antisense, 5′-CATGAGGTGGCTGCTTT-3′), CCL21a detection FITC-labeled probe (5′-CCAGGAGATCCCCCACGAACTTC-3′), and LightCycler Red 640-labeled hybrid probe (5′-AGCTGGGTGGT TCACGGT-3′); and the oligonucleotide primers specific for GAPDH (sense, 5′-TGAACGGGAAGCTCACTGG-3′; antisense, 5′-TCCACCACCCT GTTGCTGTA-3′), GAPDH detection FITC-labeled probe (5′-CTGAG GACCAGGTTGTCTCCTGCGA-3′), and LightCycler Red 640-labeled hybrid probe (5′-TTCAACAGCAACTCCCACTCTTCCACC-3′). They were designed and produced by Nihon Gene Research Laboratories.

Immunohistochemistry

For confocal microscopic analysis, the nasal tissues and intestines were fixed in 4% paraformaldehyde for the preparation of cryostat sections (5 μm) (3). These tissues were then stained with appropriate fluorescence-conjugated mAb as described above. To assess the formation of the germinal center and follicular dendritic cell (FDC) network in NALT, the previously described nasal immunization protocol was used (3). NALT sections were incubated with biotinylated peanut agglutinin (PNA) (Vector Laboratories) and then stained with FITC-streptavidin (BD Pharmingen). To detect the FDC network, the serial sections were stained with anti-FDC-M1 (BD Pharmingen) and then visualized with FITC-conjugated anti-rat IgG (BD Pharmingen). Histological analysis was performed using a confocal microscope (Leica Microsystems).

Results and Discussion

Lymphoid chemokine family-independent accumulation of CD3$^-$CD4$^+$CD45$^+$ cells at the NALT anlagen

The lymphoid chemokines CXCL13, CCL19, and CCL21 were shown to be involved in the migration of CD3$^-$CD4$^+$CD45$^+$ inducer cells into the PP anlagen (5, 6). Our previous study showed that CD3$^-$CD4$^+$CD45$^+$ inducer cells accumulated at the site of NALT development in mice aged between 7 and 10 days (3). When these lymphoid chemokine-deficient mice were examined, we detected a cluster of the inducer cells at the site of NALT formation in the infant nasal cavity of 10-day-old CXCL13$^{-/-}$ mice, *plt/plt* mice, and CXCL13$^{-/-}$*plt/plt* mice in addition to 10-day-old C57BL/6 and BALB/c mice (Fig. 1*A*). The size of the CD3$^-$CD4$^+$ inducer cell cluster in the NALT anlagen of CXCL13$^{-/-}$ infant mice and *plt/plt* infant mice was similar to that observed in control C57BL/6 and BALB/c mice, respectively. When single-cell preparations from nasal tissues of 10-day-old CXCL13$^{-/-}$ mice, 10-day-old *plt/plt* mice, and 10-day-old CXCL13$^{-/-}$*plt/plt* infant mice were examined, CD3$^-$CD4$^+$CD45$^+$ cells were also found (Fig. 2*A*). The number of CD3$^-$CD4$^+$CD45$^+$ cells isolated from nasal tissues of CXCL13$^{-/-}$ mice, *plt/plt* mice, and CXCL13$^{-/-}$*plt/plt* mice did not differ significantly from that of controls (Fig. 2*B*). As one might expect based on the previous study (6), several cellular clusters of CD3$^-$CD4$^+$ inducer cells were observed in the intestine of 17-day-old embryos (E17) of C57BL/6 and BALB/c mice (Fig. 1*B*). In contrast, we could not detect any signs of an accumulation of CD3$^-$CD4$^+$ inducer cells in intestines isolated from E17 CXCL13$^{-/-}$ mice and CXCL13$^{-/-}$*plt/plt* mice (Fig. 1*B*). These results confirm those of a previous study (6) and indicate that the degree to which the initiation of tissue genesis depends on lymphoid chemokines can be used to distinguish NALT inducer cells (NALTi) (independent) from PP inducer cells (PPi) (dependent). Thus, CXCL13 is indispensable for the accumulation of CD3$^-$CD4$^+$CD45$^+$ PPi but not of NALTi in the respective tissue anlagen.

Unexpectedly, the accumulation of inducer cells was also observed in the mesentery of E17 CXCL13$^{-/-}$ mice and CXCL13$^{-/-}$*plt/plt* mice, indicating that CXCL13 is not essential for the formation of mesenteric LN (MLN), the other member of GALT (Fig. 1*C*). Furthermore, the development of MLN was conserved in CXCR5$^{-/-}$ mice and CXCR5$^{-/-}$CCR7$^{-/-}$ mice (7). Even among GALT, then, the migration of CD3$^-$CD4$^+$ cells into the specific tissue anlagen (e.g., PP and MLN) shows a variable dependence on CXCL13. Surprisingly, FACS analysis revealed that CD3$^-$CD4$^+$CD45$^+$ cells were observed in mononuclear cells isolated from E17 intestines of CXCL13$^{-/-}$ mice, *plt/plt* mice, and CXCL13$^{-/-}$*plt/plt* mice (Fig. 2*A*). The number and the

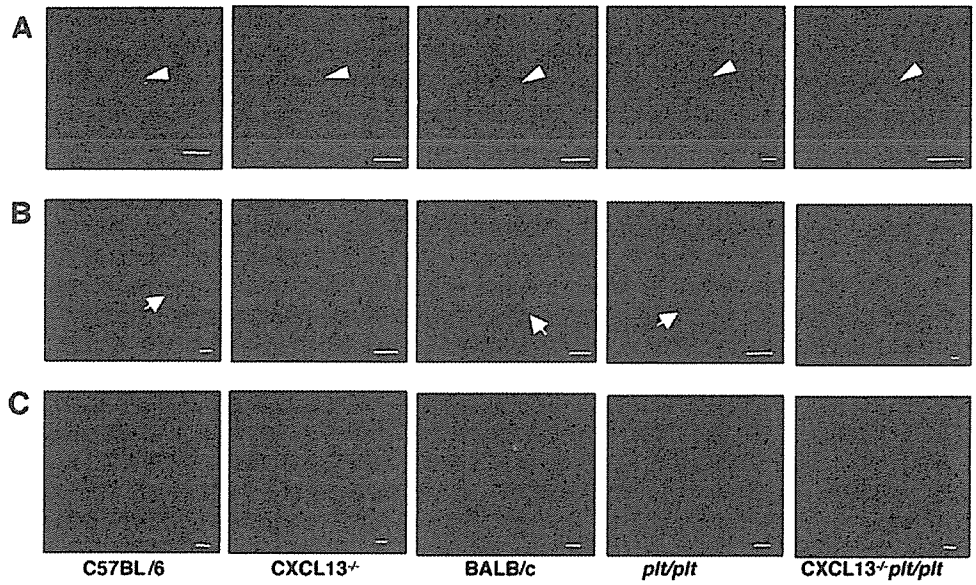

FIGURE 1. Histological analysis of infant nasal tissues and fetal intestines in lymphoid chemokine-null mice. *A*, Nasal tissues were isolated from 10-day-old C57BL/6, CXCL13$^{-/-}$, BALB/c, *plt/plt*, and CXCL13$^{-/-}$*plt/plt* mice. *B*, Fetal intestine was isolated from E17 of C57BL/6, CXCL13$^{-/-}$, BALB/c, *plt/plt*, and CXCL13$^{-/-}$*plt/plt* mice. *C*, Mesenteries were isolated from E17 C57BL/6, CXCL13$^{-/-}$, BALB/c, *plt/plt*, and CXCL13$^{-/-}$*plt/plt* mice. Frozen sections were incubated with anti-mouse CD3ε-FITC (green) and anti-mouse CD4-PE (red). Arrowheads in *A* and arrows in *B* indicate the accumulation of CD3$^-$CD4$^+$ cells at the anlagen of NALT and PP, respectively. Scale of bars, 100 μm.

frequency of CD3$^-$CD4$^+$CD45$^+$ cells in CXCL13$^{-/-}$ and *plt/plt* embryonic intestines did not differ significantly from those observed in control mice (Fig. 2). These results indicate that the migration of CD3$^-$CD4$^+$CD45$^+$ cells into embryonic intestine does not depend on lymphoid chemokines; however, CXCL13 is essential for directing the inducer cells at the site of PP anlagen.

These data demonstrate that CD3$^-$CD4$^+$CD45$^+$ NALTi can migrate to the site of NALT formation without lymphoid chemokines such as CXCL13, CCL19, and CCL21, which are known to be associated with the other lymphoid tissue genesis programs. Furthermore, the size of the CD3$^-$CD4$^+$CD45$^+$ cell cluster and the number of CD3$^-$CD4$^+$CD45$^+$ cells in infant nasal tissues did not change in lymphoid chemokine-deficient mice. Thus, the PP genesis-associated lymphoid chemokines may not have any involvement in the formation of the NALT anlagen operated by the NALTi. If that is the case, then our efforts should be focused on identifying the molecules that are at work in the migration of NALTi to the NALT anlagen.

The expression of chemokine receptors by NALTi

Inasmuch as the chemokine receptor family of CXCR5 and CCR7 has been shown to play a key role in the migration of PPi to the tissue genesis site (5), it was logical to next examine the use of the chemokines by NALTi. We first performed quantitative RT-PCR to examine the levels of CXCR5 and CCR7 expression by NALTi and PPi. For both chemokine receptors, levels expressed by NALTi were significantly lower than those expressed by PPi (Fig. 3*A*). Thus, CXCR5 and CCR7 expression by NALTi fell to levels that were barely detectable. The finding was further confirmed by FACS analysis, where PPi expressed CXCR5 and CCR7, especially the CD4^{high} fraction (Fig. 3*B*). However, NALTi expressed neither CXCR5 nor CCR7 (Fig. 3*B*).

The interaction of CXCR5/CXCL13 essentially promotes chemotactic activity for the clustering of PPi in the embryonic intestine (5). Furthermore, together with IL-7Rα signaling, CXCR5 is involved in the induction of LTα1β2 expression on PPi (7). In addition, CXCR5 signaling mediates the activation of β_1 integrin expressed on PPi for the interaction of VCAM-1$^+$ICAM-1$^+$ stromal cells at the PP anlagen (6). Although the multipotent function of CXCR5 expressed by PPi is required to initiate the development of PP, NALTi did not express CXCR5. Therefore, NALTi is thought to mediate the initiation of NALT organogenesis without a CXCR5/CXCL13-mediated signal. Furthermore, CCR7 expressed on CD3$^-$CD4$^+$CD45$^+$ cells are cooperatively involved in the organogenesis of PP and other LN (5, 7). Given that neither CCR7 nor CXCR5 is expressed on NALTi (Fig. 3, *A* and *B*), it is likely that the initial step of NALT organogenesis is completely independent of the lymphoid chemokine signaling mediated by the corresponding receptors of CXCR5 and CCR7.

Uniqueness in the production of lymphoid chemokines by NALT

To further support our findings using immunohistological analysis of the lymphoid tissue genesis in lymphoid chemokine-deficient mice, CXCL13-specific mRNA was rarely produced at the site of NALT formation of newborn and 7-day-old BALB/c and C57BL/6 mice (Fig. 3*C*). Likewise, the production of CCL19-specific mRNA at NALT anlagen was nil or extremely low in newborn mice. In contrast, we detected constitutive mRNA expression of CCL21 at the site of NALT development in mice newly born up to mice aged 6 wk (Fig. 3*C*). High levels of mRNA expression for CXCL13, CCL19, and CCL21 were also detected in the NALT of 6-wk-old mice (Fig. 3*C*). As NALT developed, the expression of lymphoid chemokines, including CXCL13 and CCL19, gradually increased.

CXCL13 and CCL19 have been shown to be produced by VCAM-1$^+$ICAM-1$^+$ stromal cells in the anlagen of PP (5). LTβR signaling through the alternative NF-κB pathway by the interaction of stromal cells and PPi is thought to induce CXCL13, CCL19, and CCL21 expression (2). In the case of NALT, neither CXCL13 nor CCL19 was expressed at birth, but the expression of both gradually increased as NALT matured. Thus, it is interesting to postulate that the initial triggering of CXCL13 and CCL19 production is induced by the cluster of NALTi accumulated at the NALT anlagen in the neonatal stage, with lymphoid cells gradually taking over the expression of these two chemokines.

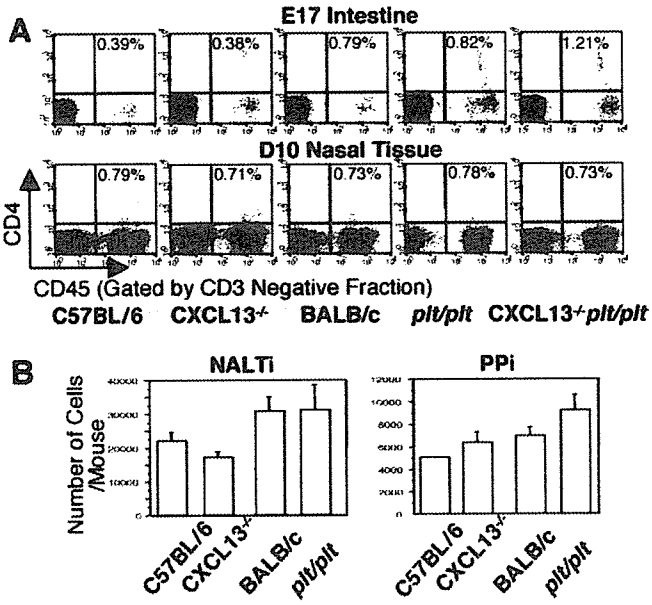

FIGURE 2. Analysis of inducer cells of lymphoid chemokine-null mice. Mononuclear cells were isolated from nasal tissues of 10-day-old mice and intestines of E17 mice. *A*, FACS analysis was performed to detect $CD3^-CD4^+CD45^+$ cells in C57BL/6, $CXCL13^{-/-}$, BALB/c, *plt/plt*, and $CXCL13^{-/-}$*plt/plt* mice. Results are representative of three independent experiments. *B*, The number of $CD3^-CD4^+CD45^+$ cells in day 10 (D10) nasal tissues (NALTi) and E17 intestines (PPi) in C57BL/6, $CXCL13^{-/-}$, BALB/c, and *plt/plt* mice. No significant differences were noted between lymphoid chemokine-null ($CXCL13^{-/-}$ and *plt/plt* mice) and control (C57BL/6 and BALB/c) mice. Significance was evaluated by an unpaired *t* test.

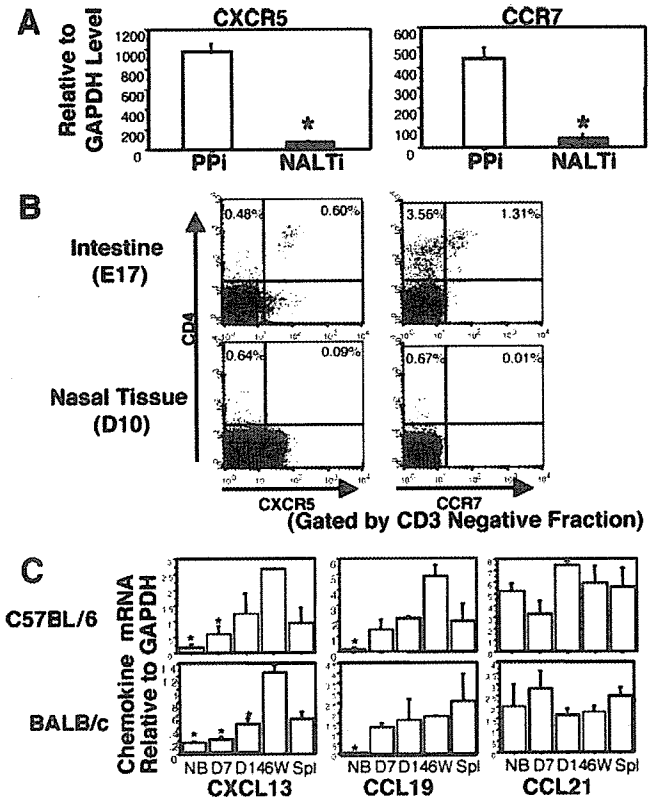

FIGURE 3. Analysis of the expressions of lymphoid chemokines and their corresponding receptors by NALTi and PPi and NALT anlagen. *A*, $CD3^-CD4^+CD45^+$ cells were sorted from mononuclear cells of day 10 (D10) nasal tissues (NALTi) and of E17 intestines (PPi) by FACSAria. Quantitative analysis of CXCR5 and CCL7 mRNA expression was performed using LightCycler. The expression of each chemokine receptor was normalized to the expression of GAPDH. RNA was extracted from three individual experiments per group. Significance was evaluated by an unpaired *t* test. *, $p < 0.05$. *B*, CXCR5 and CCR7 expression of $CD3^-CD4^+$ cells of D10 nasal tissues and E17 intestines were analyzed using FACSCalibur. *C*, Chronological analysis of lymphoid chemokine expression in NALT was performed using NALT anlagen of newborn (NB), 7-day-old (D7), and 14-day-old (D14) mice, NALT, and spleen of 6-wk-old (6W) C57BL/6 and BALB/c mice, which were isolated by a LMD system. Quantitative analysis of mRNA expression of lymphoid chemokines (CXCL13, CCL19, and CCL21) was performed using LightCycler. *, $p < 0.05$ compared with 6 wk via an unpaired *t* test ($n = 3$ on each time point).

CCL21 is produced by stromal cells in the T cell area, endothelial cells of high endothelial venules, and lymphatic vessels (7). Therefore, since the level of CCL21 expression is high at birth and remains high during the maturation stage related to the other two chemokines, stromal cells and endothelial cells in NALT, including anlagen and adult stages, seem to be a key source for the production of CCL21.

Microarchitecture of NALT in the lymphoid chemokine-null mice

Thus far, our data have demonstrated that the lymphoid chemokines CXCL13, CCL19, and CCL21 are not involved in the induction of NALT organogenesis. The role of lymphoid chemokines for the maintenance of mature NALT in adult mice should be investigated next. The total number of mononuclear cells in NALT of young adult $CXCL13^{-/-}$ mice and *plt/plt* mice was always lower than in normal mice (Fig. 4*A*). Of the various lymphoid cell subsets, the population of $B220^+$ B cell saw the greatest decrease, followed by $CD3^+$ cells and $CD11c^+$ cells in the NALT of $CXCL13^{-/-}$ mice (Fig. 4*A*). Furthermore, we sought to determine whether the migration of B1 and B2 cells into NALT might be altered in $CXCL13^{-/-}$ mice since the most obvious alteration was associated with the B cell subset. The level of CXCR5 expression by B1 cells in NALT was similar to that by B2 cells (our unpublished data). Although it has been established that a major subset of NALT B cells belong to B2 cells (13), both B1 and B2 cells were reduced in the NALT of $CXCL13^{-/-}$ mice (our unpublished data). These data indicate that CXCL13 is required for the migration of both B1 and B2 cells into NALT. Using confocal microscopic analysis, we further showed that the microarchitecture of the B cell area was destroyed in $CXCL13^{-/-}$ mice, leaving the NALT extensively occupied by T cells (Fig. 4*B*). The formation of a germinal center and FDC network was thus disrupted in the NALT of $CXCL13^{-/-}$ mice (Fig. 4*B*). In contrast, the T cell area was not observed in the NALT of *plt/plt* mice (Fig. 4*B*). The formation of the germinal center and the FDC network was intact in the NALT of *plt/plt* mice (Fig. 4*B*). These findings suggest that CXCL13 is involved in the recruitment of lymphocytes into NALT instead of the initiation of NALT tissue genesis. Furthermore, it was previously suggested that CXCL13 contributed to the subsequent microarchitecture formation of the B cell zone in NALT (9). However, it should be noted that B cell themselves are also capable of regulating the microarchitecture formation via the use of LT family-mediated signals (8). $LT\alpha1\beta2$-expressing B cells themselves promote the formation of follicles in secondary lymphoid organs (8). Therefore, B cell migration into NALT may also affect the disorganized follicles in the NALT of $CXCL13^{-/-}$ mice. In contrast, CCL19 and CCL21 preferentially promoted T cell migration into NALT